Journal of Plant Development Sciences
Meerut, India

REVIEW ARTICLE

A REVIEW ON APPLICATIONS OF UAV-BASED REMOTE SENSING FOR MAPPING SALINE AND WATERLOGGED SOILS: ADVANCES, CHALLENGES, AND FUTURE DIRECTIONS

Parteek[1]*, Mukesh Kumar[1], Pratibha[1], Ajay[1], Kapil[1] and Amandeep Singh[1]

Department of Soil and Water Engineering, CCS HAU Hisar
Email: parteekdhull9029@gmail.com

Received-15.03.2026, Revised-08.04.2026, Accepted-25.04.2026

Abstract: Soil plays an important role in addressing global environmental concerns, underlining the impacts of climate change, food and water security, land degradation, and habitat loss for various species. Soil salinity and waterlogging are among the most widespread forms of land degradation, posing serious threats to agricultural productivity, ecosystem stability, and global food security. High soil salinity and water logging reduces crop productivity and degrade soil structure, creating a need for their monitoring and management. The conventional method of soil sampling and groundwater observations yield reliable information at individual locations, their usefulness for mapping soil salinity and waterlogging is limited by sparse spatial coverage, high operational costs, and infrequent data collection. These constraints make it difficult to adequately represent the spatial complexity and rapid temporal changes associated with salinity and waterlogging processes. Nowadays, UAV-based remote sensing overcomes these limitations by providing high-resolution, spatially continuous, and timely information, enabling more accurate delineation and monitoring of affected areas. These platforms offer a more effective approach for accessing soil salinity and waterlogging by using different type of UAV sensor and increase the accuracy of results.

Keywords: UAV remote sensing, Hyperspectral imaging, Multispectral imaging

INTRODUCTION

Soil salinity and water logging are the major forms of land degradation which affecting agricultural productivity, ecosystem stability, and global food security. Nowadays, it is estimated that more than 800 million hectares of land worldwide are affected by salinity and water logging problems which frequently co-occurs in irrigated and poorly drained landscapes, especially in arid and semi-arid regions (FAO, 2021). These soil conditions reduce crop yields, limit root development, disrupt nutrient uptake, and accelerate land abandonment and posing significant challenges to sustainable land management.

The Traditional methods of soil salinity and water logging accessing depend heavily on field surveys, soil sampling, and laboratory analyses. Even though these methods can give accurate results at specific locations, they require significant amount of time, effort, and resources, thus making the practical use of such methods difficult to apply across large or diverse landscapes and also the measurements taken directly in the field may often fail to capture the natural variability of salinity and soil moisture, which can change considerably due to small differences in land elevation, irrigation practices, and soil texture (Corwin and Lesch, 2013). Therefore, decisions based solely on ground observations may be limited, as they do not always reflect the full range of conditions present across the entire area.

Therefore, the Satellite remote sensing has been emerged as a powerful technique which greatly improved monitoring of soil degradation from local regions to global scales. But the Satellite data are also narrowed due to low spatial resolution, atmospheric effects, low revisit periods and mixed pixel effects, at least in the discontinuous agricultural regions. Such limitations reduce the efficiency of satellite images to follow the fine or early-stage trends of salinity and waterlogging as applied in the accuracy agriculture sector.

In the recent years UAV-based remote sensing has become a strong alternative, which is capable of replacing conventional remote sensing, as a replacement connects the ground survey with the satellite survey. UAV platforms have ultra-high spatial resolution imagery, flex-bright deployment, and flexible capture of data governed by the time and space requirement of the user. The combination of UAVs with advanced sensors such as multispectral, hyper spectral, thermal, and LiDAR systems have provided new opportunities for detailed soil mapping and monitoring (Manfreda *et al.*, 2018).

Soil Salinity and Water logging: Processes and Remote Sensing Signatures

Processes Leading to Soil Salinization and Waterlogging

*Corresponding Author

The salinization of the soil takes place when soluble salts are deposited in the soil profile, which happens as a result of the occurrence of natural processes. e.g. weathering of parent material, capillary rise of saline groundwater or as a result of human activity like poor irrigation control and poor and insufficient drainage (Rengasamy, 2006). Overuse of low-quality irrigation water with high evaporation rates on top of it enhances the rate of salt accumulation in the root zone, primarily in the arid and semi-arid conditions (Qadir *et al.*, 2007).

Waterlogging refers to the state whereby the soils have their pores filled with water over extended durations rendering oxygen unavailable in the root zone. The cause of this condition is usually shallow ground water tables, heavy rainfall, flat plains and incompetently constructed irrigation or drainage systems. It is possible to describe salinity and waterlogging as the tightly related processes, as with the increase in groundwater table often bringing dissolved salts to the ground surface, increasing the salinization (Corwin, 2021).

Effects on Soil Properties and Vegetation

Salinity and waterlogging have a massive impact on the physical, chemical and biological attributes of soils. Salt causes inhibition of water uptake by plants, ion toxicity, especially of sodium and chloride ions (Munns and Tester, 2008). Sodic conditions also cause worsening of soil structure as they spread clay particles and slow down the infiltration rates. (Rengasamy & Olsson, 1991). The salinity and waterlogging effects on vegetation involve less biomass, leaf turning, slowed growth, and the change of the canopy architecture pattern. Such responses of stress directly affect the property of surface reflectance and hence vegetation is the major indirect indication used by remote sensing in detecting soil degradation. In extreme situations, bare salt crusts can be developed which results in specific spectral characteristics of the soil which can be directly mapped.

Spectral Characteristics of Saline and Waterlogged Soils

The saline soils have specific reflectance values at the visible (VIS), near-infrared (NIR), and shortwave infrared (SWIR) wavelengths. The salt crusts are mostly light in color, hence reflecting a lot of visible bands; whereas certain absorption in the SWIR region is attributed to the evaporite minerals like gypsum and halite (Metternicht & Zinck, 2003). These characteristics have been extensively used in hyperspectral remote sensing investigations. Conversely, waterlogged soils have a lower reflectance at the NIR region because they have more surface water and water molecules absorb the reflectance. Infrared data, especially thermal ones, can be especially useful in the detection of waterlogged lands since the surface temperatures of saturated soils decrease in relation to those of well-drained soils under the conditions of the daytime (Allbed *et al.*, 2018). The spectral and thermal analysis of the soils analyzed increases the discrimination of the saline, waterlogged, and non-affected soils.

Overview of UAV Remote Sensing Technology

UAV Platforms for Soil Mapping

UAV platforms used in environmental and agricultural monitoring are generally classified as fixed-wing or multirotor systems. Fixed-wing UAVs are capable of covering large areas efficiently and are well suited for regional surveys; however, they require more space for takeoff and landing and offer limited at low altitudes (Colomina & Molina, 2014).

Multirotor UAVs, including quadcopters and hexacopters, provide greater operational flexibility, precise hovering capability, and vertical takeoff and landing. These features make them particularly suitable for detailed soil surveys, repeated monitoring, and field-scale assessments where high spatial resolution is required. As a result, multirotor platforms dominate UAV applications in salinity and waterlogging research (Manfreda *et al.*, 2018).

Figure 1. UAV platforms: (a) Multi-rotor UAV, (b) Fixed-wing UAV, (c) Unmanned Helicopter, (d) VTOLUAV

Sensor Types Relevant to Salinity and Waterlogging Detection

UAVs can be equipped with a wide range of sensors tailored to specific mapping objectives. RGB cameras provide high spatial detail and are useful for visual interpretation and surface pattern analysis.

(a) (b) (c) (d)

Figure 2. Sensors carried by UAVs: (**a**) RGB Camera, (**b**) Multi-spectral Camera, (**c**) Hyper-spectral Camera, (**d**) LIDAR

Multispectral sensors capture discrete bands in the VIS and NIR regions and are widely used to derive vegetation and soil indices related to stress and moisture conditions (Bendig *et al.*, 2015). Multispectral sensors mounted on UAVs typically capture reflectance in key spectral bands such as blue, green, red, red-edge, and near-infrared, enabling the derivation of indices related to vegetation stress and soil properties. Indices such as the Normalized Difference Vegetation Index (NDVI) and Soil-Adjusted Vegetation Index (SAVI) have been widely used as indirect indicators of salinity-induced crop stress, particularly in irrigated agricultural systems (Allbed & Kumar, 2013).

Hyperspectral sensors offer contiguous spectral information across hundreds of narrow bands, enabling detailed identification of salt minerals and subtle vegetation stress responses. Hyperspectral sensors provide enhanced capabilities by capturing narrow, contiguous spectral bands that allow direct identification of salt-related absorption features, especially in the shortwave infrared region. UAV-based hyperspectral imagery has demonstrated strong potential for distinguishing between different salt types and salinity severity levels, even in sparsely vegetated or bare soil conditions (Aasen *et al.*, 2018). Despite their advantages, hyperspectral systems remain constrained by higher costs, increased data complexity, and limited flight endurance. Although historically limited by cost and payload constraints, recent advances in lightweight hyperspectral sensors have increased their adoption in UAV-based soil studies (Aasen *et al.*, 2018).

Thermal infrared sensors play a crucial role in detecting waterlogged areas by measuring land surface temperature variations associated with soil moisture conditions. Saturated soils typically exhibit lower daytime surface temperatures due to higher thermal inertia and evaporative cooling, making thermal imagery particularly effective for identifying persistent waterlogged zones (Allbed *et al.*, 2018).

Thermal sensors are critical for detecting surface moisture while LiDAR provides high-resolution elevation data essential for analyzing micro-topography and drainage conditions. Elevation data derived from UAV-based photogrammetry or LiDAR further enhance waterlogging assessments by capturing micro-topographic variations that control surface runoff, ponding, and subsurface flow. The fusion of thermal and topographic data has been shown to significantly improve waterlogging detection accuracy.

UAV-Based Sensors and Data Acquisition for Saline and Waterlogged Soil Mapping

Flight Planning and Data Acquisition factors

Flight planning and data acquisition strategies are very important to ensure that UAV-based assessments of soil salinity and waterlogging are reliable. In contrast to satellite platforms, UAV surveys are very configurable and this feature enables researchers to optimize the spatial resolution, illumination conditions, and timing of the study based on the study objectives. The first factor that determines the sampling distance of the ground is the altitude of the flight, which should be chosen with care to ensure the little variability of the soil and vegetation is taken as well as ensuring that there is an efficient distribution. Flight altitudes of 30 to 120 m above the ground level have been effective in the resolution of micro-topographic features and surface patterns related to the salinity and water accumulation in most studies that were soil-oriented (Diaz-Varela *et al.*, 2015). Another essential aspect is image overlap because to have a successful photogrammetric reconstruction, high side and forward overlap is necessary. The commonly adopted overlaps of more than 70 percent in the direction of the flight and 60 percent in the lateral direction are to guarantee a reliable production of orthomosaic and elevation models. The time of UAV surveys is also significant. Flights are also normally carried out in clear sky conditions and near solar noon so that the effects of shadow and radiometric variability can be minimized. In the case of waterlogging, surveys immediately after irrigation events or rainfall can increase contrast between saturated and well-drained lands, and thus detecting

waterlogging more successfully (Manfreda *et al.*, 2018).

Image Generation and Data Preprocessing

Raw UAV imagery is not ready to be quantitatively analyzed, it requires a couple of preprocessing processes. Radiometric calibration is necessary to transform the raw digital numbers into surface reflectance values that provide a comparable value across the sensors, as well as flight dates. This is often attained with calibration panels that have known properties of reflectance or with onboard irradiance sensors that consider the varying illumination conditions (Bendig *et al.*, 2015). Effects on the atmosphere are not as high at the heights of UAV flights as they are in satellite imagery, but the variation in illumination caused by the varying solar angles and cloud cover still needs to be addressed. (Colomina & Molina, 2014).

Analytic Techniques and Modeling

In the last decade, the shift of research at the level of simple visual interpretation of UAV imagery has been towards more sophisticated quantitative and data-based research. These approaches can be primarily divided into spectral index-based approaches, machine learning-based modeling, and multi-depth salinity estimation methods that rely on combined sources of data**.**

Salinity and Waterlogging Vegetation and Soil Indices

One of the oldest and most popular methods of determining soil salinity using UAV imaging is spectral index-based. They are mathematical expressions of a series of reflectance values of various bands in the spectrum, constructed to amplify features of a particular soil or vegetation, and to reduce background noise. Saline conditions determine the accumulation of salt in the soil, which influences the color, brightness of the surface, and the physiological activities of the plants that determine spectral reflectance patterns of the UAV sensors. Many experiments have found that salinity does not only modify the chlorophyll content, the leaf structure, and the water uptake of plants, which are measurable changes in vegetation reflectance, especially in the visible spectrum, red-edge spectrum and near infrared spectrum. The bands can be used to obtain indices that can then serve as proxy measurements of soil salinity, through the effects of salt-induced vegetation stress. To detect saline patches, reflectance-based indices that are sensitive to surface brightness and soil moisture have also been utilized on bare or sparsely vegetated soils. It has been shown that salinity discriminative or stress indices may be more sensitive than traditional vegetation indices including NDVI particularly in moderately stressed crops, as opposed to entirely degraded crops. (Metternicht & Zinck, 2003). In spite of the fact that spectral indices are fairly easy to compute and interpret, their effectiveness may be affected by soil moisture, surface roughness, type of crops, and the stage of their development. Consequently, there is a lot of current literature suggesting the use of a combination of multiple indices or combining them with additional data, to enhance reliability and strength of estimating salinity**.**

Statistical and Machine Learning Models

In addition to index-based methods, statistical and machine learning models have also seen an increment in using UAV data to estimate the level of soil salinity and waterlogging. The application of spectral features as related to measured electrical conductivity or moisture content of soil has traditionally been performed through the use of linear and multiple regression models. Non-linear relationships and complicated interactions between variables are however not easy to capture with these models (Corwin and Lesch, 2013). Random forests, support vector machines and artificial neural networks are machine learning methods which have been shown to perform better when working with high-dimensional datasets as well as non-linear trends. There have been recent reports of multispectral, thermal and combination accuracy of prediction being significantly better when multispectral and thermal are used. topographic variables in the ensemble learning systems (Zhang *et al.*, 2019). The models are mostly efficient in heterogeneous agricultural landscapes with salinity and water logging that are spatially different.

Ground Truth Data and Model Validation

Good ground truth data are mandatory in the process of calibration and validation of UAV-based models. The strategies of soil sampling usually imply the measurements of electrical conductivity, pH, moisture content, and ion concentrations in the representative sites within the area of study. These field measurements also give reference data, with reference to which the estimations of UAV are checked (Qadir *et al.*, 2007). Cross-validation is widely used and independent test datasets are often used to validate the models in order to determine the robustness and generalizability of the model. There are performance measures like the coefficient of determination (R2), root mean square error (RMSE), and mean error (MAE) that are commonly results. The research continuously highlights that the precision of UAV-based salinity and waterlogging maps is highly conditioned by the quality and their spatial representativeness of ground measurements (Corwin, 2021).

Applications and Case Studies

UAV-Based Mapping of Saline Soils in Agricultural and Arid Environments

UAV-based remote sensing has been widely applied to map saline soils across irrigated agricultural systems and arid landscapes where salinization poses a persistent threat to productivity. High-resolution multispectral and hyperspectral UAV imagery has enabled detailed delineation of salinity gradients within individual fields, revealing spatial patterns

driven by irrigation practices, soil texture, and micro-topography (Allbed & Kumar, 2013). These fine-scale maps provide insights that are not achievable using conventional satellite imagery, particularly in fragmented or heterogeneous agricultural regions.

In arid and semi-arid environments, UAV hyperspectral data have proven effective for identifying surface salt crusts and evaporite deposits, even under sparse vegetation cover. Several studies have demonstrated strong correlations between UAV-derived spectral features and laboratory-measured soil electrical conductivity, confirming the reliability of UAV platforms for quantitative salinity assessment (Metternicht & Zinck, 2003; Aasen *et al.*, 2018). Such applications highlight the value of UAVs for early detection of salinity hotspots and targeted soil reclamation efforts.

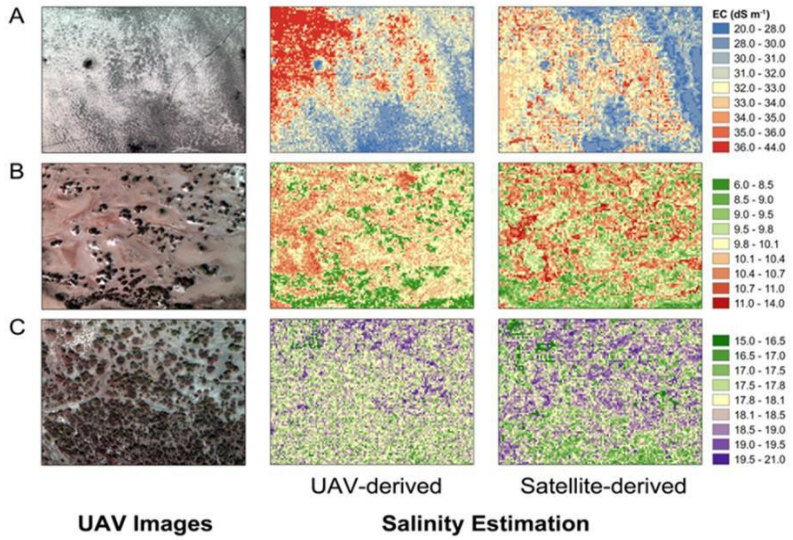

Figure 1. UAV hyperspectral images and derived soil salinity maps compared to coarser satellite-based salinity maps for three study fields (A, B, C). (Hu *et al.*, 2019)

Detection and Monitoring of Waterlogged Soils

Waterlogging detection has benefited substantially from the integration of UAV-based thermal and elevation data. Thermal imagery acquired during daytime conditions has been used to identify saturated soils through reduced land surface temperatures, enabling rapid mapping of poorly drained zones following irrigation or rainfall events (Allbed *et al.*, 2018). When combined with multispectral indicators of vegetation stress, thermal data improve discrimination between temporary surface wetness and persistent waterlogging.

Repeated UAV surveys have also facilitated temporal monitoring of waterlogging dynamics, allowing researchers to track the expansion or contraction of saturated areas across seasons. Digital elevation models derived from UAV photogrammetry have been instrumental in linking waterlogged zones to subtle topographic depressions and drainage constraints, providing actionable information for drainage design and land leveling interventions.

Advantages of UAVs Over Conventional Field Methods and Satellite Sensing for Soil Salinity and Moisture Mapping

Monitoring soil salinity and moisture is essential for understanding soil health, managing irrigation, and ensuring sustainable agricultural production. Traditionally, soil monitoring has relied on **ground-based sampling and laboratory analysis**, which, although accurate at specific points, suffer from severe limitations in spatial coverage and temporal frequency. Satellite remote sensing provides a broader perspective but has its own set of challenges. UAVs (drones), positioned between ground surveys and satellite systems, offer significant advantages for both **precision and operational flexibility**.

Higher Spatial Resolution

One of the most important advantages of UAV remote sensing is its ability to collect ultra-high spatial resolution imagery—often at sub-meter or even centimeter levels—which is crucial for capturing fine-scale variability in soil salinity and moisture. Soil salinization and moisture patterns often occur at field and sub-field scales, exhibiting patchy distributions that coarse satellite pixels (10–30 m or larger) cannot resolve accurately. Studies comparing UAV and satellite data for soil salinity show that UAV-based models significantly outperform satellite-based models in precision, often with higher coefficients of determination (e.g., R^2 ~0.89 for UAV vs R^2 ~0.63 for satellite) and lower error metrics when estimating salt distribution at field scale.

Because UAVs fly at low altitudes, they reduce the mixed-pixel problem common in satellite imagery, where one pixel may represent multiple land covers (soil, vegetation, water), which blurs the soil signal. This enhanced detail enables more accurate mapping of soil variability even in heterogeneous landscapes.

Temporal Flexibility and On-Demand Data Collection

Conventional soil surveys require intensive labor and are typically conducted infrequently, due to cost and logistical constraints. In contrast, satellites have fixed revisit periods (e.g., 5–16 days for Sentinel or Landsat), which may not align with critical soil or crop conditions such as post-irrigation infiltration, rapid salinity changes, or moisture flux after rainfall.

UAVs provide **on-demand data acquisition**, meaning they can be deployed precisely when and where needed to capture conditions at critical times, such as during drought stress, irrigation scheduling, or soil reclamation activities. This temporal flexibility makes UAVs particularly useful for monitoring dynamic processes like soil moisture changes or rapid salt movement into the root zone.

Sensor Versatility and Customization

UAVs can carry a wide range of sensors tailored to soil assessment tasks:

Multispectral sensors that capture reflectance in visible and near-infrared bands useful for vegetation and soil indices.

Hyperspectral systems with many narrow spectral bands capable of detecting subtle soil chemical differences. For example, UAV-borne hyperspectral imagery has been shown to produce more accurate soil salinity estimates (with lower RMSE and higher concordance) than satellite multispectral sources.

Thermal cameras to detect variations in surface temperature that correlate with soil moisture and water stress.

LiDAR or photogrammetry to derive precise terrain and micro-topographic information that influences water accumulation and drainage.

This range of payload options allows UAVs to gather complementary data types in a single flight mission, enabling more comprehensive soil and moisture analysis than conventional methods or satellite sensors.

Enhanced Model Accuracy through Data Fusion

Integration of UAV data with satellite imagery can improve large-area monitoring. UAV data can be used to **calibrate and upscale satellite models**, correcting the coarse satellite output and yielding higher accuracy for broad-scale soil monitoring. For instance, combining UAV-derived high-resolution data with satellite imagery improved the satellite inversion model's R^2 from 0.63 to 0.787 and increased spatial agreement with ground truth from ~76% to ~90%.

This synergy highlights how UAVs can enhance large-scale monitoring not by replacing satellites but by calibrating and supplementing them to combine high precision and wide coverage.

Cost and Operational Efficiency Compared to Conventional Field Surveys

Traditional soil salinity and moisture assessment relies on systematic ground sampling, laboratory analysis (e.g., measuring electrical conductivity), and extensive field labor. This approach is time-consuming, expensive, and difficult to repeat at high frequency.

UAV surveys, although requiring initial equipment investment, significantly reduce long-term costs for repeated monitoring. They allow large areas to be surveyed quickly with minimal human labor on the ground, which improves safety in difficult terrain and reduces operational risk. UAV systems are also easier to mobilize and can be flown at relatively low cost compared to chartering manned aircraft for aerial surveys.

Improved Sensitivity to Soil and Vegetation Interactions

UAVs excel at capturing the interaction between soil conditions and plant responses at fine scales. Soil salinity and moisture influence plant physiology, expressed through changes in canopy reflectance and temperature. UAV imagery can detect these subtle changes in vegetation indices or thermal patterns that often precede visible stress signs, enabling early detection of problematic zones for intervention or irrigation adjustments.

Challenges and Limitations

Operational and Environmental Constraints

In spite of the mentioned advantages, UAV systems have a number of operational constraints that limit its widespread use. Flight endurance and payload capacity are limited which limits its coverage range, especially when carrying hyperspectral or thermal sensors. Wind, precipitation, extreme temperatures are also sensitive factors in UAV operations that may have an impact on flight safety and quality of data (Colomina & Molina, 2014). The presence of thick vegetation cover, roughness of the surface and unstable light contribute to the further complexity of the interpretation of UAV imagery. These limitations indicate the need to pay special attention to the design of the survey and the importance of realistic expectations when it comes to the applicability of the data.

Information Processing and Technical Complexity.

UAV Imagery is high-resolution, which implies that large amounts of data produced by this method consume a lot of computing power and technical skills to process. Photogrammetric reconstruction, radiometric calibration and sophisticated modeling procedures may be slow and technically challenging. These requirements are still a major obstacle to many end users, especially the local agencies and smallholder farmers (Manfreda *et al.*, 2018). Streamlining the operations by automating, processing in the clouds and using standardized protocols is thus a significant field to be developed in the future.

Regulation and Economic Factors.

The regulatory systems in place that govern the operations of UAVs are diverse across nations and may curtail the level of altitude, range covered, and

the flexibility of operations. Flight permissions can be costly, in both time and cost, especially in cases of large scale or recurring surveys. Moreover, the prices of the UAV platforms, sensors, and specialized software, in particular, hyperspectral and thermal ones, are still prohibitive to some users (Zhang and Kovacs, 2012). These regulatory and economic considerations should be put into serious consideration when considering the feasibility of the UAV-based soil monitoring programs**.**

Future Trends and Research.

The UAV Sensor Technology Innovations.

The fast development of the technology of UAV sensors will considerably contribute to the detection and monitoring of the saline and waterlogged soils. Hyperspectral and thermal sensors with low power consumption have already been developed, increasing the payload capacity in UAVs, which allows them to take longer flights and cover a larger area (Aasen *et al.*, 2018). In the future designs of sensors, spectral resolution in the short wave infrared band will be enhanced, this is important in the direct determination of salt minerals and soil moisture dynamics. Simultaneously, the advancements in onboard GNSS and inertial measurement units will advance the accuracy of geolocation, thus allowing a more reliable multi-temporal analysis. Such technological advancements will diminish the operational limitations and expand the possibility of soil mapping using UAVs to conduct regular agricultural and environmental monitoring.

Applications of Artificial intelligence and Deep Learning.

Deep learning and artificial intelligence are becoming one of the transformative tools of UAV-based mapping of soil conditions. Artificial intelligence systems can also detect intricate spatial and spectral features, such as salinity and waterlogging, in high-resolution images with deep learning models and identify all these features on different terrains without having to be trained to generate these features by humans (Zhang *et al.*, 2019). Deep learning, in comparison to conventional machine learning methods, provides a more flexible way to process raw imagery and multi sensor data fusion. Nevertheless, these approaches present emerging issues on data needs and computational and model interpretability. Future studies are required on how to create transferable models that are reliably operating across regions, seasons, and explainable AI solutions which enhance transparency and user confidence. These concerns will be crucial to the process of making operational tools out of methodological advances.

Cloud based platforms and real time processing

Another new trend with considerable prospects of operational use is the integration of UAV systems with real-time data processing and cloud-based systems. The development of edge computing and wireless data transmission is allowing the creation of near-real-time orthomosaics and analytical products, minimizing the gap between the collection of information and the decision-making process (Manfreda *et al.*, 2018). Data sharing, collaboration, and scalability are also facilitated by the cloud-based processing platforms to enable the use of UAV-obtained soil maps by bigger agricultural decision-support systems. These advancements are specialized especially to the early warning systems to reduce risks of salinity and waterlogging in case of climate variability.

Precision Agriculture/Land Management Implications.

Saline and water-logged soil mapping by UAVs has immense application in decision-support of precision agriculture. The high-resolution spatial data allows site-specific irrigation scheduling, drainage design, and the application of amendments in the soil, which minimize the input costs and the negative effects of the environment at the same time. Focusing on the areas of impact, farmers will be able to maximize the efficiency of resource utilization and productivity (Corwin, 2021). At more macro scales, the UAV-products are applicable in the land management, policy formulation since the products are timely and precise in informing about the pattern of soil degradation. UAV-based early warning mechanisms can be used to provide prior action before disaster strikes to minimize the economic losses in the long run and help in the sustainable intensification. When incorporated into the local land management systems, UAV technology will increase transparency, accountability, and decision-making that is evidence-based.

CONCLUSIONS

This review has synthesized recent advances in UAV-based remote sensing for mapping and monitoring saline and waterlogged soils, highlighting significant progress in sensor technology, analytical methods, and practical applications. UAV platforms offer unparalleled spatial resolution, operational flexibility, and multi-sensor integration capabilities that address key limitations of conventional field surveys and satellite remote sensing.

The reviewed literature demonstrates that UAV-based approaches are highly effective for detecting fine-scale salinity gradients and waterlogging patterns, particularly when multispectral, hyperspectral, thermal, and topographic data are combined with machine learning models. Despite remaining challenges related to cost, regulation, and data processing complexity, ongoing technological and methodological innovations are rapidly expanding the operational viability of UAV systems.

Overall, UAV-based remote sensing represents a transformative tool for soil degradation assessment and management. Its continued integration into precision agriculture and sustainable land management strategies will be essential for

addressing the growing challenges of soil salinity and water logging in a changing climate

REFERENCES

Aasen, H., Burkart, A., Bolten, A. and Bareth, G. (2018). Generating 3D hyperspectral information with lightweight UAV snapshot cameras for vegetation monitoring. *Remote Sensing of Environment*, **204**: 12-25.

Google Scholar

Allbed, A. and Kumar, L. (2013). Soil salinity mapping and monitoring in arid and semi-arid regions using remote sensing technology: A review. *Advances in Remote Sensing*, **2**(4): 373-385.

Google Scholar

Allbed, A., Kumar, L. and Aldakheel, Y. (2018). Assessing soil salinity using soil salinity and vegetation indices derived from IKONOS high spatial resolution imagery. *Remote Sensing* **10**(1): 1-20.

Google Scholar

Bendig, J., Bolten, A. and Bareth, G. (2015). UAV-based imaging for multi-temporal, very high-resolution crop surface models to monitor crop growth variability. *Photogrammetrie-Fernerkundung-Geoinformation*, **6**: 551-562.

Google Scholar

Colomina, I. and Molina, P. (2014). Unmanned aerial systems for photogrammetry and remote sensing: A review. *ISPRS Journal of Photogrammetry and Remote Sensing*, **92**: 79-97.

Google Scholar

Corwin, D.L. (2021). Climate change impacts on soil salinity in agricultural systems. *European Journal of Soil Science*, **72**(2): 842-862.

Google Scholar

Corwin, D.L. and Lesch, S.M. (2013). Application of soil electrical conductivity to precision agriculture: Theory, principles and guidelines. *Agronomy Journal*, **95**(3): 455-471.

Google Scholar

Díaz-Varela, R.A., De la Rosa, R., León, L. and Zarco-Tejada, P.J. (2015). High-resolution airborne UAV imagery to assess olive tree crown parameters using 3D photo reconstruction. *Remote Sensing*, **7**(4): 4213-4232.

Google Scholar

Food and Agriculture Organization of the United Nations (2021). *Global map of salt-affected soils*. FAO, Rome.

Google Scholar

Manfreda, S., McCabe, M.F., Miller, P.E., Lucas, R., Pajuelo Madrigal, V., Mallinis, G. and Toth, B. (2018). On the use of unmanned aerial systems for environmental monitoring. *Remote Sensing*, **10**(4): 641.

Google Scholar

Metternicht, G. and Zinck, J.A. (2003). Remote sensing of soil salinity: Potentials and constraints. *Remote Sensing of Environment*, **85**(1): 1-20.

Google Scholar

Munns, R. and Tester, M. (2008). Mechanisms of salinity tolerance. *Annual Review of Plant Biology*, **59**: 651-681.

Google Scholar

Qadir, M., Boers, T.M., Schubert, S., Ghafoor, A. and Murtaza, G. (2007). Agricultural water management in saline environments. *Agricultural Water Management*, **90**(1-2): 2-16.

Google Scholar

Qadir, M., Quillérou, E., Nangia, V., Murtaza, G., Singh, M., Thomas, R.J., Drechsel, P. and Noble, A.D. (2014). Economics of salt-induced land degradation and restoration. *Natural Resources Forum*, **38**(4): 282-295.

Google Scholar

Rengasamy, P. (2006). World salinization with emphasis on Australia. *Journal of Experimental Botany*, **57**(5): 1017-1023.

Google Scholar

Rengasamy, P. (2010). Soil processes affecting crop production in salt-affected soils. *Functional Plant Biology*, **37**(7): 613-620.

Google Scholar

Rengasamy, P. and Olsson, K.A. (1991). Sodicity and soil structure. *Australian Journal of Soil Research*, **29**(6): 935-952.

Google Scholar

Zhang, C. and Kovacs, J.M. (2012). The application of small unmanned aerial systems for precision agriculture: A review. *Precision Agriculture*, **13**(6): 693-712.

Google Scholar

Zhang, Y., Li, M., Zheng, L., Qin, Q. and Liu, Y. (2019). UAV-based multispectral imagery for salinity mapping using machine learning. *Remote Sensing*, **11**(18): 2195.

Google Scholar

Journal of Plant Development Sciences
Meerut, India

RESEARCH ARTICLE

ANGIOSPERMIC PLANT DIVERSITY OF VIKRAMSHILA GANGETIC DOLPHIN WILDLIFE SANCTUARY, BHAGALPUR, BIHAR, INDIA

Onkar Nath Maurya[1]* and Tanay Shil[2]

Botanical Survey of India, CGO Complex, 3rd MSO Building, Block F, 5th Floor, DF Block, Sector 1, Salt Lake City, Kolkata-700064

[2]Central National Herbarium, Botanical Survey of India, Howrah-711103, West Bengal, India

**Corresponding author Email: onmaurya@bsi.gov.in*

Received-20.03.2026, Revised-11.04.2026, Accepted-26.04.2026

Abstract: This study presents the first comprehensive survey of flowering plant diversity within the Vikramshila Gangetic Dolphin Wildlife Sanctuary, situated in Bhagalpur district, Bihar, India. The investigation documents 163 species of angiosperms representing 138 genera and 51 families, along with details on their habits and phonological periods.

Keywords: Vikramshila Gangetic Dolphin Wildlife Sanctuary, Floristic diversity, Angiosperms

INTRODUCTION

The Vikramshila Gangetic Dolphin Wildlife Sanctuary in Bhagalpur district was established in 1990 to protect the endangered Gangetc Dolphin (*Platanista gangetica gangetica* Roxb.), which is listed in the IUCN Red List (Das & Maurya, 2015). Early floristic records from Bhagalpur were documented by Haines (1921–1925) in 'Botany of Bihar and Orissa'. The Dicot flora of the district was later explored by Verma (1981). Studies on algal diversity from nearby regions were conducted by several researchers, including Singh & Saha (1982a, 1982b), Saha & Pandit (1986, 1987), Saha & Wuzek (1989), Kumar & Saha (1993), Kargupta & Jha (2004). Additional floristic data of Bhagalpur were included in 'Flora of Bihar-Analysis' (Singh et al., 2001). Das & Maurya (2015), documented algal flora of Vikramsila Gangetic Dolphin Sanctuary (Bihar) for the first time with a record of sixty five taxa including 13 taxa of Cyanophyceae of 11 genera, 24 taxa of Chlorophyceae of 15 genera, 21 taxa of Bacillariophyceae of 16 genera, 5 taxa of Euglenophyceae of 1 genus and one taxa each under Dinophyceae and Xanthophyceae. Maurya *et al.*(2015) reported *Bromelia pinguin* L.(Bromeliaceae) for first time in India from this sanctuary. However, no comprehensive study on angiosperm diversity has been reported from the sanctuary until now. Therefore, the present work explores and documents the flowering plant diversity of this protected area for the first time to assess its botanical wealth.

Study area

The study area is Vikramshila Gangetic Dolphin Wildlife Sanctuary located in Bhagalpur district of Bihar, India. It is a 60 km gangetic stretch from Sultanganj (25° 25′ N 86° 73′ E) and Kahalgaon (25° 28′ N 87° 22′ E).

*Corresponding Author

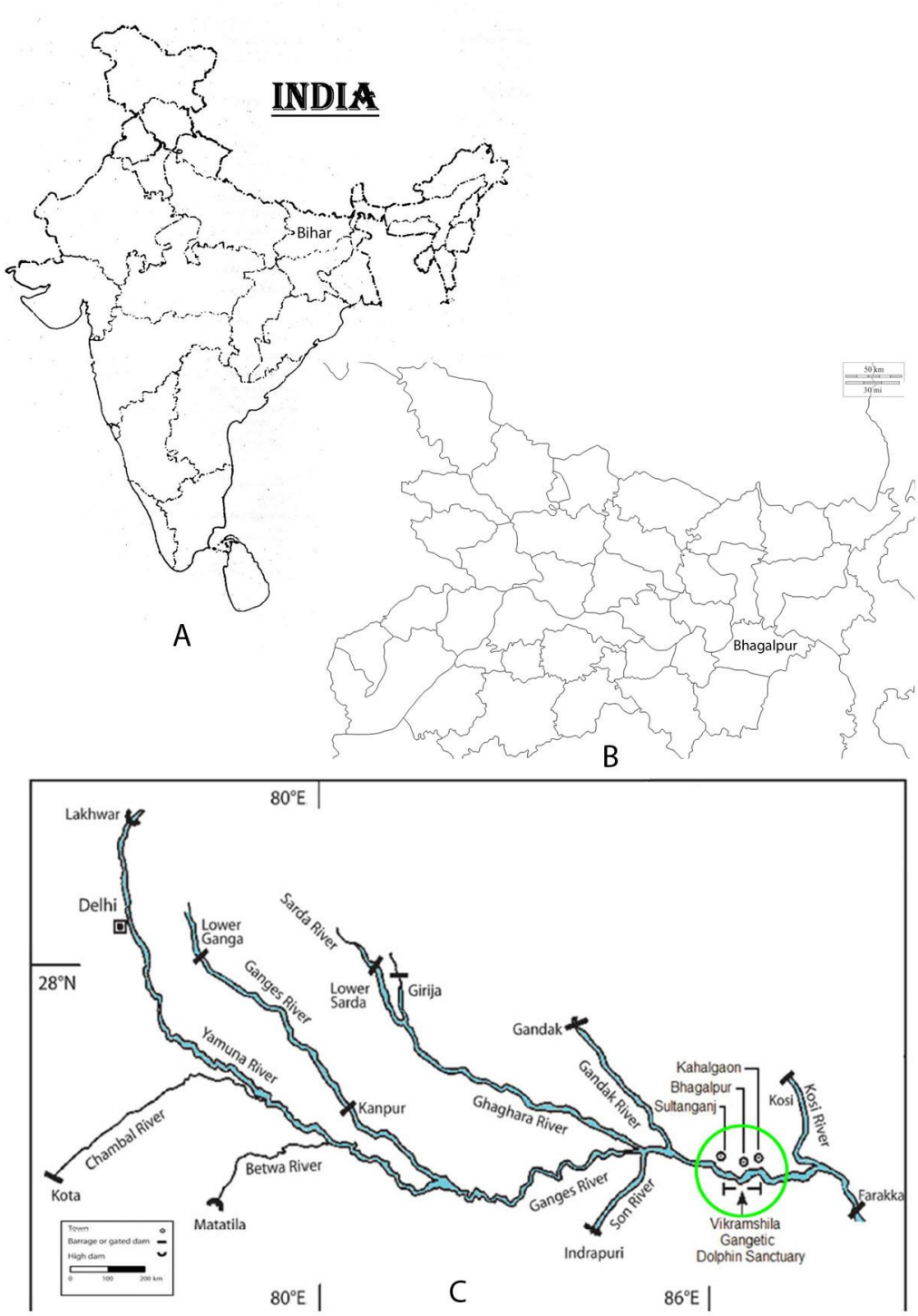

Fig: Map of Vikramsila Gangetic Dolphin Wildlife Sanctuary and collection sites

MATERIALS AND METHODS

Plant samples were collected for two years from March 2013 to September 2016. Freshly collected specimens were worked out and identified with the help of standard keys from relevant floras, monographs and were reconfirmed by matching them with the authentic specimens present in Central National Herbarium (CAL). Voucher specimens are deposited in Central National Herbarium (CAL). The nomenclature of plants has been updated using Plants of the World Online (2025) and International Plant Name Index (2025).

RESULTS AND DISCUSSION

Table 1. Enumerates the flowering plant diversity identified in Vikramhsila Gangetic Dolphin Wildlife Sanctuary.

Table 1. Checklist of Angiosperms of Vikramshila Gangetic Dolphin Wildlife Sanctuary, Bhagalpur, Bihar, India

Sl no.	Plant names	Family	Phenology	Habit	Specimen examined
1.	*Nymphaea nouchali* Burm.f.	Nymphaeaceae	Sept.–Nov.	Herb	*ONM* 62359, 67959
2.	*Polyalthia suberosa* (Roxb.) Thwaites	Annonaceae	Major part of the year	Tree	*ONM* 62387, 63964
3.	*Litsea suberosa* Yen C. Yang & P.H. Huang	Lauraceae	June – Oct.	Shrub	*ONM* 63916
4.	*Typhonium trilobatum* (L.) Schott	Araceae	April – Sept.	Herb	*ONM* 63935
5.	*Hydrilla verticillata* (L.f.) Royle	Hydrocharitaceae	April – Dec.	Herb	*ONM* 67902
6.	*Najas graminea* Delile		Aug. – Oct.	Herb	*ONM* 67965
7.	*Vallisneria spiralis* L.		Jan. - May	Herb	*ONM* 63999
8.	*Potamogeton crispus* L.	Potamogetonaceae	Nov. – Apr.	Herb	*ONM* 62400
9.	*Potamogeton nodosus* Poir.		Aug. – May	Herb	*ONM* 62345
10.	*Commelina benghalensis* L.	Commelinaceae	July – Nov.	Herb	*ONM* 62237
11.	*Cyanotis axillaris* (L.) D.Don ex Sweet		Aug. – Jan.	Herb	*ONM* 62223, 62239
12.	*Pontederia crassipes* Mart.	Pontederiaceae	May – Sept.	Herb	ONM 62210, 63924
13.	*Bromelia pinguin* L.	Bromeliaceae	Feb. - May	Herb	*ONM* 63949
14.	*Cyperus difformis* L.	Cyperaceae	Aug. – Dec.	Herb	*ONM* 62309, 63997
15.	*Cyperus iria* L.		Aug. – Jan.	Herb	*ONM* 62244, 67957
16.	*Cyperus michelianus* (L.) Delile		March – Dec.	Herb	*ONM* 62369, 67929
17.	*Cyperus rotundus* L.		July – Dec.	Herb	*ONM* 62228, 62281, 62293, 62372, 67949
18.	*Fimbristylis aestivalis* Vahl		Sept. – Nov.	Herb	*ONM* 62288, 62370
19.	*Fimbristylis littoralis* Gaudich.		Aug. – Oct.	Herb	*ONM* 62246
20.	*Schoenoplectiella lateriflora* (J.F.Gmel.) Lye		Aug. – Nov.	Herb	*ONM* 63995, 63996
21.	*Cynodon dactylon* (L.) Pers.	Poaceae	Throughout the year	Herb	*ONM* 62340
22.	*Dactyloctenium aegyptium* (L.) Willd.		Aug. – March	Herb	*ONM* 62280
23.	*Dactyloctenium aristatum* Link		July – Oct.	Herb	*ONM* 62374
24.	*Desmostachya bipinnata* (L.) Stapf		May – Nov.	Herb	*ONM* 63955
25.	*Dichanthium annulatum* (Forssk.) Stapf		Aug. – Nov.	Herb	*ONM* 62397
26.	*Digitaria ciliaris* (Retz.) Koeler		Aug. – Nov.	Herb	*ONM* 62241, 62262,
27.	*Echinochloa colona* (L.) Link		July – Dec.	Herb	*ONM* 62282, 63993, 67923,
28.	*Echinochloa stagnina* (Retz.) P.Beauv.		Aug. – Dec.	Herb	*ONM* 63994
29.	*Eleusine indica* (L.) Gaertn.		June – Nov.	Herb	*ONM* 62245
30.	*Panicum repens* L.		July – Dec.	Herb	*ONM* 62355, 63950
31.	*Paspalidium flavidum* (Retz.) A.Camus		June – Nov.	Herb	*ONM* 62263
32.	*Paspalum scrobiculatum* L.		July – Dec.	Herb	*ONM* 62243
33.	*Phalaris minor* Retz.		Feb. – March	Herb	*ONM* 62363
34.	*Phragmites karka* (Retz.) Trin. ex Steud.		July – Dec.	Herb	*ONM* 62211

35.	*Saccharum spontaneum* L.		Aug. – Nov.	Herb	*ONM* 62212, 62296
36.	*Setaria verticillata* (L.) P.Beauv.		Sept. – Oct.	Herb	*ONM* 62242, 62307
37.	*Sorghum bicolor* (L.) Moench		Aug. – Oct.	Herb	*ONM* 62270
38.	*Sorghum halepense* (L.) Pers.		Oct. – Dec.	Herb	*ONM* 62226, 62247, 67921
39.	*Argemone mexicana* L.	Papavaraceae	Dec. - May	Herb	*ONM* 63919, 67919
40.	*Fumaria vaillantii* Loisel.		Nov. - March	Herb	*ONM* 67934
41.	*Cocculus hirsutus* (L.) W.Theob.	Menispermaceae	Nov. - April	Climber	*ONM* 63985
42.	*Tiliacora acuminata* (Lam.) Miers		April - June	Climber	*ONM* 63941, 67070
43.	*Tinospora sinensis* (Lour.) Merr.		Feb. - June	Climber	*ONM* 63912
44.	*Ranunculus sceleratus* L.	Ranunculaceae	Nov. - March	Herb	*ONM* 62308, 62353
45	*Cayratia trifolia* (L.) Domin	Vitaceae	April – Dec.	Climber	*ONM* 62216, 63913, 67953
46.	*Canavalia gladiata* (Jacq.) DC.	Fabaceae	Sept. – Dec.	Climber	*ONM* 67913
47.	*Grona triflora* (L.) H.Ohashi & K.Ohashi		Throughout the year	Herb	*ONM* 62264
48.	*Guilandina bonduc L.*		July – April	Shrub	*ONM* 67932
49.	*Pleurolobus gangeticus* (L.) J.St.-Hil. ex H.Ohashi & K.Ohashi		June – Jan.	Herb	*ONM* 67976, 67981
50.	*Senna sophera* (L.) Roxb.		Aug. – Dec.	Herb	*ONM* 67908
51.	*Sesbania sesban* (L.) Merr.		Throughout the year	Herb	*ONM* 62208, 67927
52.	*Cannabis sativa* L.	Cannabaceae	Feb. - April	Herb	*ONM* 62318
53.	*Trema orientale* (L.) Blume		Throughout the year	Tree	*ONM* 63917, 63978
54.	*Artocarpus lacucha* Buch.-Ham.	Moraceae	March – Aug.	Tree	*ONM* 63947
55.	*Ficus hispida* L.f.		Throughout the year	Tree	*ONM* 62389, 63922
56.	*Coccinia grandis* (L.) Voigt	Cucurbitaceae	March – Dec.	Climber	*ONM* 62248, 63908, 63986, 67977
57.	*Oxalis corniculata* L.	Oxalidaceae	Throughout the year	Herb	*ONM* 62305
58.	*Passiflora foetida* L.	Passifloriaceae	Major part of the year	Climber	*ONM* 63911
59.	*Breynia vitis-idaea* (Burm.f.) C.E.C.Fisch.	Euphorbiaceae	Aug. – Nov.	Shrub	ONM 62217
60.	*Croton bonplandianum* Baill.		All the year round	Herb	*ONM* 67943
61.	*Euphorbia hirta* L.		All the year round	Herb	*ONM* 62235, 62300, 67962
62.	*Euphorbia hypericifolia* L.		Major part of the year	Herb	*ONM* 63965
63.	*Mallotus repandus* (Willd.) Müll.Arg.		Dec. – Apr.	Tree	*ONM* 63975
64.	*Phyllanthus reticulatus* Poir.		Throughout the year	Shrub	*ONM* 67966
65.	*Phyllanthus virgatus* G.Forst.		July - March	Herb	*ONM* 62375, 63906, 67904, 67965
66.	*Ricinus communis* L.		Major part of the year	Shrub	*ONM* 62388

67.	*Combretum indicum* (L.) DeFilipps	Combretaceae	Major part of the year	Climber	*ONM* 67922
68.	*Ammannia baccifera* L.	Lythraceae	July – Feb.	Herb	*ONM* 62310, 67928
69.	*Ludwigia perennis* L.	Onagraceae	Aug. – Dec.	Herb	*ONM* 62304
70.	*Cardiospermum halicacabum* L.	Sapindaceae	May – Nov.	Climber	*ONM* 62291, 63910
71.	*Glycosmis pentaphylla* **(**Retz.) DC.	Rutaceae	Throughout the year	Herb	*ONM* 62276, 62358
72.	*Abutilon indicum* (L.) Sweet	Malvaceae	Aug. - March	Herb	*ONM* 62257, 62283, 62338, 63974, 67973
73.	*Malvastrum coromandelianum* (L.) Garcke		Major part of the year	Herb	*ONM* 62395, 67979
74.	*Melochia corchorifolia* L.		Aug. – Nov.	Herb	*ONM* 62225
75.	*Pentapetes phoenicea* L.		Aug. – Dec.	Herb	*ONM* 63991
76.	*Sida cordata* (Burm.f.) Borss.Waalk.		All the year round	Herb	*ONM* 62320
77.	*Urena lobata* L.		Aug. - March	Herb	*ONM* 62261, 62279, 67974
78.	*Capparis zeylanica* L.	Capparaceae	Oct. - April	Shrub	*ONM* 63946
79.	*Cleome viscosa* L.		Almost throughout the year	Herb	*ONM* 62254, 67969
80.	*Crateva religiosa* G.Forst.		March - July	Tree	*ONM* 63940, 67968
81.	*Loranthus longiflorus* Desr.	Loranthaceae	Nov. - April	Shrub	*ONM* 67918
82.	*Persicaria hydropiper* (L.) Delarbre	Polygonaceae	Throughout the year	Herb	*ONM* 63989
83.	*Polygonum plebeium* R.Br.		Major part of the year	Herb	*ONM* 62303, 62335
84.	*Rumex maritimus* L.		Nov. - March	Herb	*ONM* 62329
85.	*Polycarpon prostratum* (Forssk.) Asch. & Schweinf.	Caryophyllaceae	Feb. - May	Herb	*ONM* 68845
86.	*Achyranthes aspera* L.	Amaranthaceae	All the year round	Herb	*ONM* 62272
87.	*Alternanthera philoxeroides* (Mart.) Griseb.		March – May	Herb	*ONM* 62203, 62294, 62378,
88.	*Alternanthera sessilis* (L.) R.Br. ex DC.		Throughout the year	Herb	*ONM* 62206, 62220, 62267
89.	*Amaranthus spinosus* L.		Throughout the year	Herb	*ONM* 62231
90.	*Amaranthus viridis* L.		All the year round	Herb	*ONM* 62230, 62277
91.	*Celosia argentea* L.		Aug. – Feb.	Herb	*ONM* 63990
92.	*Cyathula prostrata* (L.) Blume		Aug. – Dec.	Herb	*ONM* 67972
93.	*Deeringia amaranthoides* (Lam.) Merr.		Sept. – Jan.	Shrub	*ONM* 67916
94.	*Digera muricata* (L.) Mart.		Throughout the year	Herb	*ONM* 62274, 63936, 67914, 67960
95.	*Dysphania ambrosioides* (L.) Mosyakin & Clemants		April – Aug.	Herb	*ONM* 63920
96.	*Pupalia lappacea* (L.) Juss.		Aug. - March	Herb	*ONM* 67909
97.	*Boerhavia diffusa* L.	Nyctaginaceae	Aug. – March	Herb	*ONM* 62259
98.	*Boerhavia repens* L.		Aug. – Jan.	Herb	*ONM* 67967

99.	*Glinus oppositifolius* (L.) Aug.DC.	Molluginaceae	Almost throughout the year	Herb	*ONM* 62364, 63943, 63954
100.	*Anagallis arvensis* L.	Primulaceae	Dec. - March	Herb	*ONM* 62298, 62324
101.	*Dentella repens* (L.) J.R.Forst. & G.Forst.	Rubiaceae	Throughout the year	Herb	*ONM* 62368, 63376, 63925
102.	*Neolamarckia cadamba* (Roxb.) Bosser		May – Dec.	Tree	*ONM* 63933
103.	*Centaurium pulchellum* (Sw.) Druce	Gentianaceae	Aug. – Sept.	Herb	*ONM* 62346, 62347
104.	*Calotropis gigantea* (L.) Dryand.	Apocynaceae	Most part of the year	Shrub	*ONM* 62249
105.	*Calotropis procera* (Aiton) Dryand.		Feb. - July	Shrub	*ONM* 63963
106.	*Oxystelma esculentum* (L. f.) Sm.		Sept. – Nov.	Climber	*ONM* 62207, 67946,
107.	*Pergularia daemia* (Forssk.) Chiov.		April – Oct.	Climber	*ONM* 62256, 63976, 67956
108.	*Rauvolfia serpentina* (L.) Benth. ex Kurz		April – Sept.	Herb	*ONM* 63937, 67971
109.	*Telosma pallida* (Roxb.) W. G. Craib		May – Jan.	Climber	*ONM* 63938
110.	*Cordia myxa* L.	Boraginaceae	August – Nov.	Tree	*ONM* 63945
111.	*Heliotropium indicum* L.		Major part of the year	Herb	*ONM* 63915, 67944, 62332, 62289
112.	*Cuscuta reflexa* Roxb.	Convolvulaceae	Oct. - March	Herb	*ONM* 62306
113.	*Evolvulus nummularius* (L.) L.		July – Feb.	Herb	*ONM* 62222, 62354, 63926, 67978
114.	*Ipomoea aquatica* Forssk.		Throughout the year	Herb	*ONM* 62202, 62292, 62391, 63987, 67951
115.	*Ipomoea carnea* Jacq.		Throughout the year	Shrub	*ONM* 62201, 67948
116.	*Merremia emarginata* (Burm. f.) Hallier f.		Sept. – Dec.	Herb	*ONM* 62218, 67901, 67963
117.	*Merremia hederacea* (Burm. f.) Hallier f.		Oct. – Dec.	Herb	*ONM* 62209
118.	*Operculina turpethum* (L.) Silva Manso		Dec. - March	Climber	*ONM* 62285, 67911
119.	*Datura metel* L.	Solanaceae	All the year round	Shrub	*ONM* 63914, 63973, 67958,
120.	*Datura stramonium* L.		Aug. – Dec.	Shrub	*ONM* 62250
121.	*Nicotiana plumbaginifolia* Viv.		Throughout the year	Herb	*ONM* 62319, 63909, 67945
122.	*Physalis minima* L.		Aug. – Dec.	Herb	*ONM* 67925
123.	*Solanum nigrum* L.		Throughout the year	Herb	*ONM* 62266
124.	*Solanum verbascifolium* L.		Major part of the year	Herb	*ONM* 67917
125.	*Solanum violaceum* Ortega		All the year round	Shrub	*ONM* 62316
126.	*Solanum virginianum* L.		Major part of the year	Herb	*ONM* 63928, 63952
127.	*Jasminum sambac* (L.) Aiton	Oleaceae	April - July	Herb	*ONM* 63932, 63959
128.	*Mecardonia procumbens* (Mill.) Small	Plantaginaceae	All the year round	Herb	*ONM* 63365

129.	*Scoparia dulcis* L.		All the year round	Herb	*ONM* 62367, 63939, 67980
130.	*Lindernia crustacea* (L.) F.Muell.	Linderniaceae	July - March	Herb	*ONM* 62224, 62295
131.	*Lindernia hyssopoides* (L.) Haines		Nov. - April	Herb	*ONM* 67931
132.	*Vandellia crustacea* (L.) Benth.		July – Dec.	Herb	*ONM* 67964
133.	*Verbascum chinense* (L.) Santapau		Jan. - May	Herb	*ONM* 62330, 63944
134.	*Hygrophila polysperma* (Roxb.) T.Anderson	Acanthaceae	Nov. - March	Herb	*ONM* 62339, 63971
135.	*Peristrophe bicalyculata* (Retz.) Nees		Oct. - April	Herb	*ONM* 63981
136.	*Ruellia prostrata* Poir.		July – Dec.	Herb	*ONM* 62238, 62342, 63921
137.	*Rungia pectinata* (L.) Nees		Throughout the year	Herb	*ONM* 67915
138.	*Rungia repens* (L.) Nees		Oct. – Feb.	Herb	*ONM* 63910
139.	*Utricularia aurea* Lour.	Lentibulariaceae	Oct. – Jan.	Herb	*ONM* 62356, 63972
140.	*Lantana camara* L.	Verbenaceae	Throughout the year	Shrub	*ONM* 63982, 67961
141.	*Lippia alba* (Mill.) N.E.Br. ex Britton & P.Wilson		Throughout the year	Shrub	*ONM* 62348, 67950
142.	*Phyla nodiflora* (L.) Greene		All the year round	Herb	*ONM* 62224, 62314
143.	*Vitex negundo* L.		All the year round	Shrub	*ONM* 63918, 67955
144.	*Anisomeles indica* (L.) Kuntze	Lamiaceae	Major part of the year	Herb	*ONM* 62255, 62286
145.	*Clerodendrum inerme* (L.) Gaertn.		Nov. - March	Shrub	*ONM* 63930
146.	*Clerodendrum infortunatum* L.		Jan. - May	Shrub	*ONM* 62331
147.	*Leucas aspera* (Willd.) Link		All the year round	Herb	*ONM* 62251
148.	*Leucas cephalotes* (Roth) Spreng.		July – Dec.	Herb	*ONM* 62302
149.	*Nepeta hindostana* (B.Heyne ex Roth) Haines		Oct. – March	Herb	*ONM* 62343, 63984
150.	*Salvia plebeia* R.Br.		Dec. – June	Herb	*ONM* 62357
151.	*Nymphoides indica* (L.) Kuntze	Menyanthaceae	March – Nov.	Herb	*ONM* 62349, 67903
152.	*Ageratum conyzoides* (L.) L.	Asteraceae	Throughout the year	Herb	*ONM* 62301
153.	*Caesulia axillaris* Roxb.		Aug. – Feb.	Herb	*ONM* 67930
154.	*Chromolaena odorata* (L.) R.M.King & H.Rob.		Nov. - March	Herb	*ONM* 63983
155.	*Cirsium arvense* (L.) Scop.		Jan. - April	Herb	*ONM* 62323
156.	*Cyanthillium cinereum* (L.) H.Rob.		All the year round	Herb	*ONM* 62278
157.	*Eclipta prostrata* (L.) L.		Throughout the year	Herb	*ONM* 62229, 62265, 62287, 62325, 63905, 67952
158.	*Grangea maderaspatana* (L.) Poir.		Dec. - June	Herb	*ONM* 62299, 62334, 63904
159.	*Pseudognaphalium luteoalbum* (L.) Hilliard & B.L.Burtt		Feb. - April	Herb	*ONM* 62312, 62350
160.	*Spilanthes calva* DC.		Aug. – Feb.	Herb	*ONM* 62271, 62337

161.	*Synedrella nodiflora* (L.) Gaertn.		Sept. – Jan.	Herb	*ONM* 62275, 67975
162.	*Tridax procumbens* (L.) L.		All the year round	Herb	*ONM* 62253
163 .	*Xanthium strumarium* L.		Sept. - May	Herb	*ONM* 62290

A total of 163 species of angiosperms belonging to 138 genera of 51 families are recorded. Dicotyledones comprise 43 families, 110 genera and 128 species and monocotyledons comprise 8 families, 28 genera and 35 species respectively. Dicotyledonous and monocotyledonous comprises 79 % and 21 % of the total species respectively.

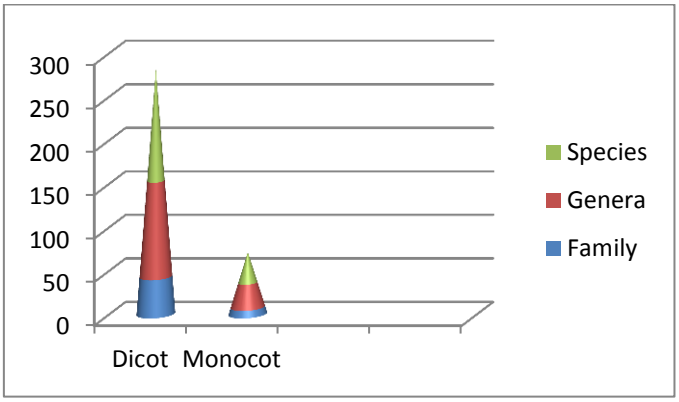

Fig: Dicot and Monocot Species with respect to Family, Genera and Species

Floristic study reveals that Poaceae, the most dominant family is represented by 16 genera and 18 species followed by Asteraceae (12 genera and 12 species) and Amaranthaceae (9 genera and 11 species). The three dominant families of Vikramshila Gangetic Dolphin Wildlife Sanctuary comprise 41 species. Out of 51 families, 26 families are represented by a single genus with a single species.
The plants are grouped into 4 categories (Herb, Shrub, Climber, and Tree) based on their habit. Herb, shrub, climber, and tree comprises 75%, 12%, 8%, and 5% and of total number of species respectively.

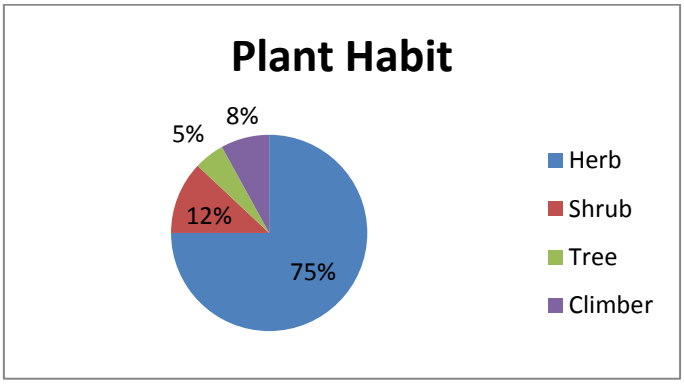

Fig: Habit of the Plant Species

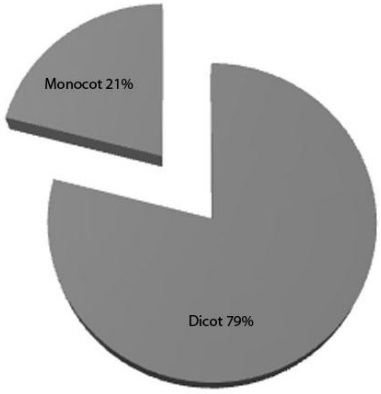

Fig: Distribution of dicot and monocot species

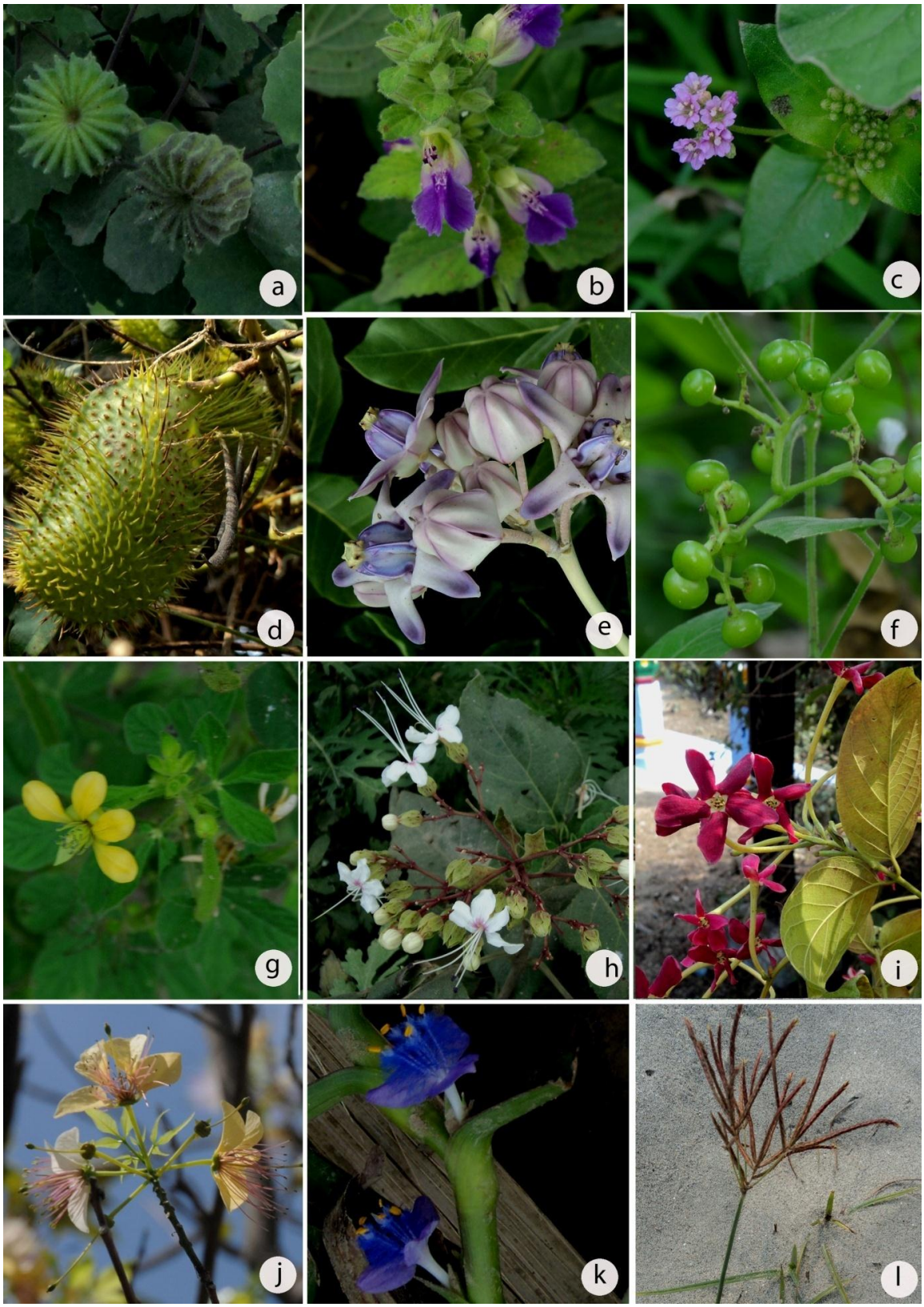

Plate 1: a. *Abutilon indicum* (L.) Sweet; b. *Anisomeles indica* (L.) Kuntze; c. *Boerhavia diffusa* L.; d. *Caesalpinia bonduc* (L.) Roxb.; e. *Calotropis gigantea* (L.) Dryand.; f. *Cayratia trifolia* (L.) Domin; g. *Cleome viscosa* L.; h. *Clerodendrum infortunatum* L.; i. *Combretum indicum* (L.) DeFilipps j. *Crateva religiosa* G.Forst.; k. *Cyanotis axillaris* (L.) D.Don ex Sweet; l. *Cyperus rotundus* L.

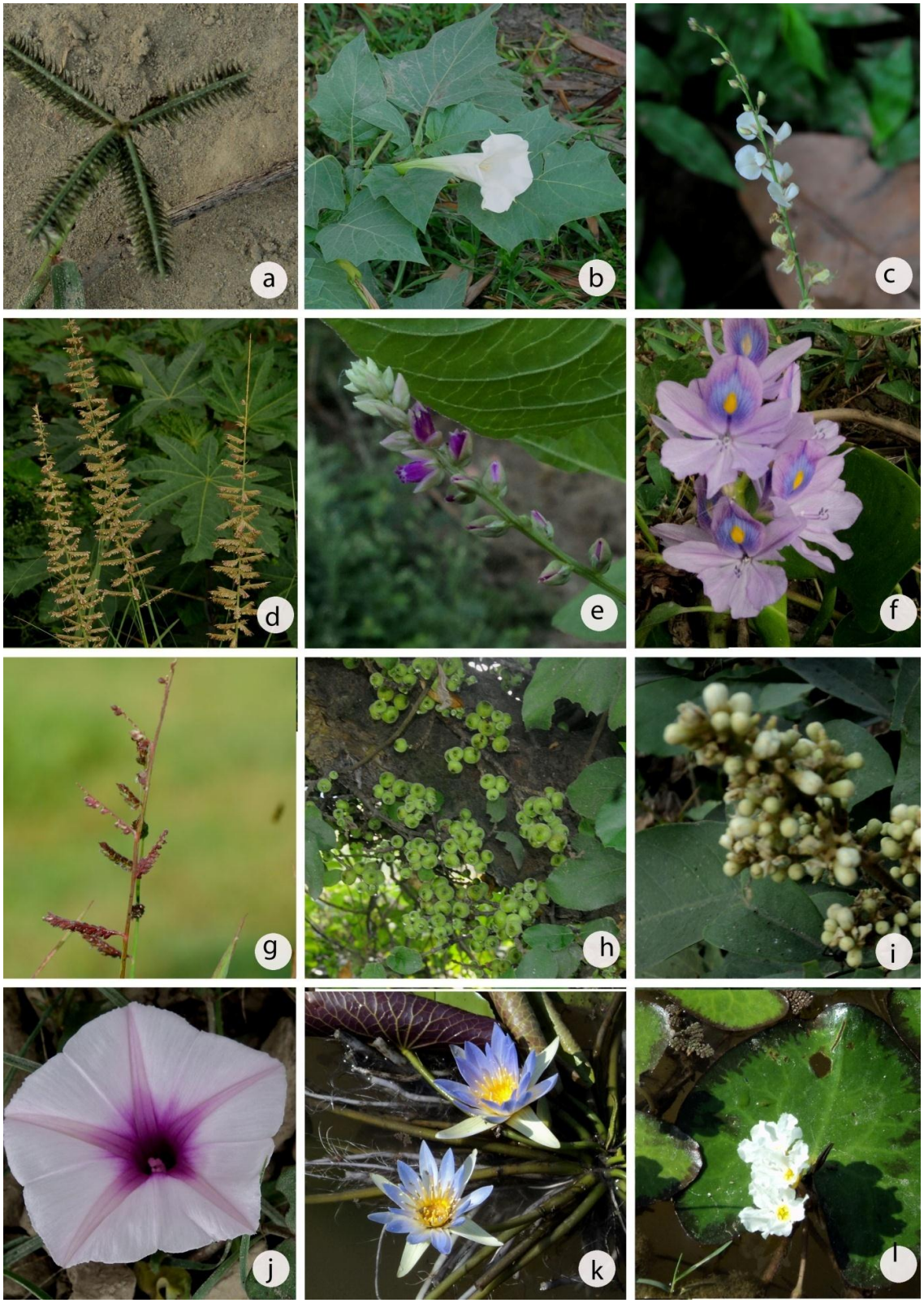

Plate 2: a. *Dactyloctenium aegyptium* (L.) Willd.; b. *Datura metel* L.; c. *Desmodium gangeticum* (L.) DC.; d. *Desmostachya bipinnata* (L.) Stapf; e. *Digera muricata* (L.) Mart.; f. *Eichhornia crassipes* (Mart.) Solms; g. *Echinochloa colona* (L.) Link; h. *Ficus hispida* L.f.; i. *Glycosmis pentaphylla* (Retz.) DC.; j. *Ipomoea aquatica* Forssk.; k. *Nymphaea nouchali* Burm.f.; l. *Nymphoides indica* (L.) Kuntze

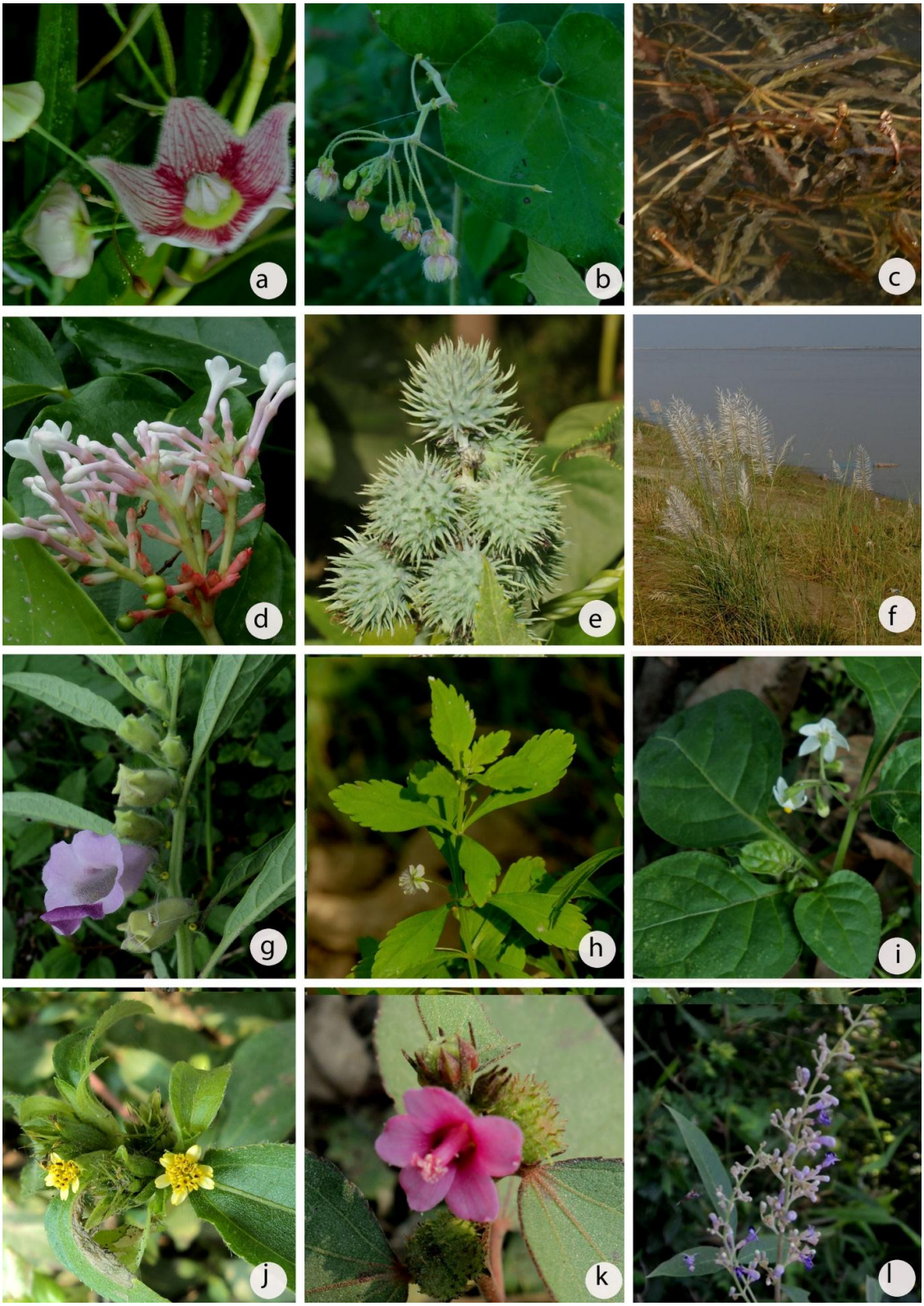

Plate 3: a. *Oxystelma esculentum* (L. f.) Sm.; b. *Pergularia daemia* (Forssk.) Chiov.; c. *Potamogeton crispus* L.; d. *Rauvolfia serpentina* (L.) Benth. ex Kurz; e. *Ricinus communis* L.; f. *Saccharum spontaneum* L.; g. *Sesamum indicum* L.; h. *Scoparia dulcis* L.; i. *Solanum nigrum* L.; j. *Synedrella nodiflora* (L.) Gaertn.; k. *Urena lobata* L.; l. *Vitex negundo* L.

CONCLUSION

The present study highlights the angiospermic plant diversity of Vikramshila Gangetic Dolphin Wildlife Sanctuary, Bhagalpur, Bihar which is extensively documented. Occurrence of 163 species indicate a well represented angiosperms diversity.

ACKNOWLEDGEMENT

The authors are thankful to the Director, Botanical Survey of India, Kolkata and Scientist–F and Head of Office, Central National Herbarium, Botanic Garden, Howrah for providing necessary facilities.

REFERENCES

Das, S. and Maurya, O.N. (2015). Floristic survey of Algae in Vikramshila Gangetic Dolphin Sanctuary, Bihar (India). *Nelumbo* **57**: 124–134.
Google Scholar

Haines, H. H. (1921–1925). Botany of Bihar and Orissa (Rep. 1961). Botanical Survey of India, Calcutta.
Google Scholar

International Plant Name Index. International PlantNames Index (IPNI). Royal Botanic Gardens, Kew,2021. Available from: https://www.ipni.org/ (accessed: 3rd Nov. 2025)
Google Scholar

Kargupta, A.N. and Jha, R.N. (2004). *Algal flora of Bihar (Zygnemataceae)*. Bishen Singh Mahendra Pal Singh, Dehradun.
Google Scholar

Kumar, S. and Saha, L.C. (1993). Fresh water algae of drinking water reservoirs at Bhagalpur. *Phykos* **32**: 131–146.
Google Scholar

Maurya, Onkar Nath; **Kumar, Anand; Krishna, G. &Halder, S.** (2015) On the Occurrence of a non-native plant species *Bromelia penguin* L. (Bromeliaceae) in India, *Phytodiversity* **2**(1):32-38.
Google Scholar

Saha, L.C. and Pandit, B. (1986). Periphytonic succession in a perennial pond. *J. Curr. Biosci.* **3**: 34–36.
Google Scholar

Saha, L.C. and Pandit, B. (1987). Pond and riverine algae of Bhagalpur. *Phykos* **26**: 152–158.
Google Scholar

Saha, L.C. and Wujek, D.E. (1989). Phytoplankton distribution in an oligotrophic pond and a eutrophic pond. *Acta Hydrochem. Hydrobiol.* **17**: 407–416.
Google Scholar

Singh, N.K. and Saha, L.C. (1982a). Diatoms of Bhagalpur ponds – I, Bihar. *Phykos* **21**: 128.
Google Scholar

Singh, N.K. and Saha, L.C. (1982b). Chlorococcales of Bhagalpur – 1, Bihar. *J. Econ. Taxon. Bot.* **3**: 197–200.
Google Scholar

Singh, N.P., Mudgal, V., Khanna, K.K., Srivastava, S.C., Sahoo, A.K., Bandapadhyay, S., Aziz, N., Das, M., Bhattacharya, R.P. and Hajra, P.K. (2001). Flora of Bihar: Analysis. Botanical Survey of India, Calcutta, pp. 559–561.
Google Scholar

Verma, S.K. (1981). Flora of Bhagalpur (Dicotyledons). Today and Tomorrow Print and Publishers, New Delhi.
Google Scholar

Journal of Plant Development Sciences
Meerut, India

RESEARCH ARTICLE

OPTIMIZING VEGETATIVE PROPAGATION OF THE ENDANGERED MEDICINAL HERB *VALERIANA JATAMANSI* JONES THROUGH NAPHTHALENE ACETIC ACID (NAA)

Aftab Ahmed, Suhail Shabir, Mubashir Ahmad Mir, Mohsin Bashir, Arzan Nazir and Amarjeet Singh*

Division of Forest Products and Utilization, Faculty of Forestry, Sher-e-Kashmir University of Agricultural Sciences and Technology of Kashmir, Srinagar, J&K, India
Email: amerjeetskuast@gmail.com

Received-27.03.2026, Revised-14.04.2026, Accepted-27.04.2026

Abstract: *Valeriana jatamansi* Jones, commonly known as Indian Valerian, is a critically endangered medicinal herb in the Himalayan region due to habitat loss and the overexploitation of its aromatic rhizomes for pharmaceutical use. Traditional propagation methods via seeds and rhizome division are often inefficient, characterized by poor viability and germination rates having slow growth cycle. To address this, a study was conducted at the SKUAST-K Faculty of Forestry using a hydroponic-style system with apical cuttings treated with Naphthalene Acetic Acid (NAA) at various concentrations. The methodology involved maintaining cuttings in transparent glass beakers filled with distilled water, which was changed every two days to ensure proper oxygenation and hygiene. The research findings demonstrated that a low-concentration auxin treatment of 50 ppm NAA for a 30-minute duration (T1D1) was the most effective protocol, achieving a 100% rooting success rate. This treatment produced significantly superior results across all quantitative parameters, including an average of five roots per cutting and the average root diameter of 0.271 cm. In contrast, higher concentrations of 100 ppm and 150 ppm led to physiological stress, resulting in leaf chlorosis, tissue necrosis, and a sharp decline in rooting success. This simple and reliable vegetative propagation technique offers a scalable solution for producing high-quality, uniform planting material, supporting the urgent need for the conservation and sustainable cultivation of this endangered species.

Keywords: *Valeriana jatamansi*, Stem cuttings, NAA, Rooting, Medicinal Plants, Kashmir

INTRODUCTION

Valeriana jatamansi Jones is an important herb that belongs to the family Valerianaceae, the genus consists of over 250 species, spread across the world [1] and approximately 12 species are present in India [2]. The genus is known as 'Valerian' because of its common name. Common name of Valeriana jatamansi is Mushkbala, sugandhbala in Hindi and Tagar in Sanskrit [3] [4]. Species is gynodioecious [5] and possess pubescent stem and radical leaves with several long petioled, cordate-ovate, cauline few or much smaller entire or pinnate with hairy fruits or nearly glabrous. Flowers are white tinged with pink. Root stock thick and horizontal, aromatic and modular [6] . It is distributed from Pakistan, Afghanistan south-western china, Burma and a few parts of the Indian Himalayan range and is abundantly found at an altitude of 1300-3000m from Kashmir to Bhutan, and between 1500 and 1800 metres in the hills of Khasi and Jaintia [7]. Sexual reproduction is often hindered by low seed viability and poor germination rates, making it inefficient for large-scale production. Similarly, asexual propagation through rhizome division is restricted by a long gestation period and slow growth cycles. Keeping in view these propagation problems, this study was undertaken to evaluate the effect of Naphthalene Acetic Acid (NAA) growth hormone at various concentrations on the rooting behavior of *Valeriana jatamansi* Jones.By utilizing apical cuttings in a hydroponic setup, this research seeks to optimize rooting success and produce high-quality planting material. This approach aims to overcome traditional growth delays and support the sustainable conservation of this endangered medicinal herb.

MATERIALS AND METHODS

Study Area

The study was conducted at the Benhama Campus of the Faculty of Forestry, Sher-e-Kashmir University of Agricultural Sciences and Technology of Kashmir (SKUAST-K), situated in Ganderbal, Jammu and Kashmir. Geographically, the site is positioned at approximately 34.27latitute and 74.77longitude, nestled in the foothills of the Lar mountains at an altitudinal range of 1600 m to 1843 m above mean sea level.

*Corresponding Author

Description and Selection of Plant Material

The experimental plant, *Valeriana jatamansi* Jones (commonly known as Indian Valerian), is a high-value medicinal herb known for its aromatic roots and therapeutic compounds. Healthy and mature mother plants were identified from the medicinal plant nursery of SKUAST-K, maintained under standard agronomic practices. From these mother plants, 100 apical cuttings were harvested early in the morning to ensure optimal turgidity. Each cutting was approximately 8-10 cm in length, bearing 2–3 nodes, and freshly green in appearance. Leaves present on the lower portion of the stem were removed to avoid excessive transpiration, while upper leaves were trimmed to half of their size. The basal portion of each cutting was given a slanting cut at a 45° angle to increase the surface area for root initiation and facilitate better absorption of hormone solutions. All tools used for cutting were sterilized using 70% ethanol to prevent microbial contamination.

Preparation of Hormone Treatments

NAA solutions were freshly prepared for each treatment by first dissolving the required quantity of NAA powder in a few milliliters of ethanol (to aid dissolution) and then diluting the solution to the desired concentration with distilled water. Cuttings were divided equally into four groups corresponding to the three treatment levels. Each cutting was dipped in the respective NAA solution for a fixed duration of 30,60 and 90 minutes respectively. This treatment was chosen based on previous studies which suggested that short-term exposure to auxin at low-to-moderate concentrations promotes root initiation without causing callus formation or phytotoxicity.

Table 1. Different treatments (T1 to T9) of NAA doses (ppm) at different time durations

Treatment	NAA conc. (ppm) with durations
T1D1	50ppm+30min
T2D2	50ppm+60min
T3D3	50ppm+90min
T4D1	100ppm+30min
T5D2	100ppm+60min
T6D3	100ppm+90min
T7D1	150ppm+30min
T8D2	150ppm+60min
T9D3	150ppm+90min

Experimental Design and Setup

The experiment was laid out in a Completely Randomized Design (CRD). A total of 100 apical cuttings were utilized. These cuttings were divided into three primary hormone concentration groups (50ppm,100ppm and 150ppm)'with each concentration further subdivided into three duration intervals (30,60 and 90 minutes). Each treatment combination was replicated across multiple beakers to ensure a total count of 100 samples. Each 250 ml transparent glass beaker was filled with distilled water, serving as the rooting medium for the hydroponic-style setup. Following the respective NAA dipping treatments, the cuttings were immediately transferred into these labeled beakers.

Maintenance During the Experimental Period

The beakers were placed on an elevated surface inside the lab in shade to avoid direct sunlight and excessive heat exposure. The environmental conditions during the experiment were monitored and maintained as follows:

Temperature: Between 18°C and 25°C

Relative Humidity: 70% to 80%

Light Intensity: Diffused light under par6tial shade

Observation and Data Collection

After 30 days, each cutting was gently removed from the beaker and examined for root formation. Care was taken not to damage the fragile roots during handling.

The following quantitative parameters were recorded for each rooted cutting:

Rooting Percentage (%): The proportion of cuttings in each treatment that successfully produced roots. It was calculated using the formula:

Rooting Percentage = (Number of rooted cuttings/Total number of cuttings) ×100 Number of Roots per Cutting:

Total number of adventitious roots produced per rooted cutting. The count was taken visually for each rooted sample and averaged for each treatment.

Root Length (cm): The length of the longest root on each cutting was measured using a measuring scale. This parameter reflects the growth potential and vigor of the newly formed roots.

Root Diameter (mm): The thickness of the root was measured at the widest point of the primary root using a digital vernier calliper. This parameter gives an idea about the strength and quality of root formation.

All observations were recorded in a tabulated format, and average values were calculated for each treatment and replicate.

Statistical Analysis

The experimental data were subjected to Analysis of Variance (ANOVA) using OPSTAT software developed by CCS Haryana Agricultural University, Hisar. The statistical model followed was that of a Completely Randomized Design (CRD). Treatment means were compared using the Critical Difference (CD) at 5% level of significance ($P<0.05$) to assess whether differences among the NAA concentrations were statistically significant. If the F-test was significant, the CD values were used to separate treatment means. Tables were also generated to visually represent the variation among treatments.

RESULTS AND DISCUSSION

The present investigation on **"Optimizing Vegetative Propagation of the Endangered Medicinal Herb *Valeriana jatamansi* jones Through Naphthalene Acetic Acid (NAA)"** was carried out to assess the effect of different concentrations of Naphthalene Acetic Acid (NAA) on rooting behaviour under hydroponic conditions.

Rooting Percentage

Rooting percentage is a critical indicator of successful vegetative propagation, reflecting the ability of plant tissues to initiate root primordia in response to hormonal stimuli. Among the treatments tested, the highest rooting percentage (100%) was recorded in cuttings treated with 50 ppm NAA for 30minutes (T1D1). In contrast, a steep decline in rooting success was observed in higher concentrations—66.67% for both 100 ppm (T4) and 150 ppm (T7), and a further reduction to 33.33% and complete failure in other treatments (T8-T9) as shown in table 2. This finding strongly indicates that *Valeriana jatamansi* Jones exhibits maximum rooting efficiency at lower auxin concentrations. The success of 50 ppm NAA in inducing root formation aligns with the findings of Gautam *et al.,* (2021) [8], who reported enhanced rooting at similar auxin concentrations in *Valeriana jatamansi* Jones.

On the other hand, the reduced rooting percentage at 100 ppm and 150 ppm suggests hormonal imbalance or phytotoxicity at elevated auxin levels. This phenomenon has been previously described by Klerk *et al.,* (1999) [9] , who noted that excess auxin interferes with cellular differentiation and leads to callus formation or necrosis rather than organized root development. The results confirm the presence of a hormonal threshold, beyond which auxins shift from being stimulatory to inhibitory.

Number of Roots per Cutting

In addition to root initiation, the number of roots per cutting determines the plant's ability to establish effectively after transplantation. The study found that 50 ppm NAA for 30 minutes (T1D1) produced a significantly higher number of roots (mean = 5), while T2 (100 ppm) and T3 (150 ppm) recorded mean values of 1.11 and 1.22, respectively as mentioned in table 3. The reduced number of roots in T4 and T3 may be attributed to overstimulation of auxin receptors, leading to abnormal cell division or suppression of root primordia formation. This corroborates with Hartmann *et al.,* (2011) [10], who emphasized the principle of optimal hormonal dosage for effective root induction and proliferation. Bhatt *et al.,* (2021) [11] further confirmed that excessive NAA concentrations can lead to callus tissue rather than differentiated root structures. The findings of this study are thus in strong agreement with the broader literature, reinforcing the necessity of fine-tuning auxin levels during vegetative propagation.

Figure 1: Image showing rooting in *Valeriana jatamansi* Jones cuttings.

Root Length

Root length is a key physiological trait that reflects the plant's capacity to explore the rooting medium. While occasional longer roots were observed in T3, the overall mean root length was highest in 50ppm NAA for 30 minutes (T1D1) (0.63 cm), suggesting that lower auxin concentration led to more uniform and healthier root development as shown in table 4. In T2 and T3, root elongation was inconsistent, and roots appeared thinner and weaker, indicating stress-induced elongation rather than true physiological growth. Baskaran and Jayabalan (2005) [12] reported similar findings in medicinal plants, where optimal auxin levels led to well-developed root systems,

while higher concentrations disrupted normal elongation and vascular differentiation. It is also noteworthy that high concentrations of NAA sometimes result in elongation of individual roots due to hormonal stress, but such roots often lack structural integrity and functional efficiency. T1, on the other hand, exhibited balanced development in both root length and number.

Root Diameter

Root diameter provides insight into the structural and vascular quality of the root system. Well-developed roots with higher diameters are more likely to survive transplantation, withstand desiccation, and support the shoot system. In the present study, as shown in table 5, T1 (50 ppm NAA for 30min) recorded the greatest mean root diameter (0.271 cm), indicating superior vascular development. T2 and T3 treatments showed a reduction in root diameter, with some roots appearing fragile and underdeveloped. These results support the earlier observations of [Klerk *et al.,* (1999) [9]; Baskaran and Jayabalan (2005)] [12] that emphasize the importance of balanced auxin levels for anatomical development in roots.

Table 3. Effect of NAA Concentrations on Rooting Parameters of *Valeriana jatamansi* Jones

S.No.	Treatment	Average Roots/Cutting	Average Root Length(cm)	Average Root Diameter(cm)	Rooting Percentage (%)
01	T1D1	5.00	0.630	0.271	100.00
02	T2D2	1.11	1.144	1.099	63.64
03	T3D3	1.22	1.277	0.106	63.64
04	T4D1	1.10	0.303	0.140	36.36
05	T5D2	0.00	0.077	1.110	0.00
06	T6D3	1.10	0.060	0.047	36.36
07	T7D1	1.20	0.257	0.230	36.36
08	T8D2	0.00	0.123	0.087	0.00
09	T9D3	0.00	0.00	0.00	0.00
CD (p>0.05	Factor A	0.850	0.247	0.051	
	Factor B	0.850	0.247	0.051	
	A x B	1.480	N.S	0.088	

Visual and Practical Observations

In addition to numerical parameters, visual assessments played a vital role in evaluating treatment effectiveness. The cuttings under 50 ppm NAA for 30 minutes (T1D1) appeared greener, turgid, and free from symptoms of stress throughout the 30-day observation period. In contrast, cuttings in higher concentration treatments began to show leaf chlorosis, wilting, callus formation, and tissue necrosis, especially in T3.

Role of NAA Concentration and Exposure Time

The effectiveness of 50 ppm NAA concentration is largely attributed to its ability to stimulate endogenous auxin activity without disrupting the natural hormonal balance within the plant. The 30-minute exposure time was short enough to allow absorption without over saturating the tissues. Studies have shown that excessive auxin concentrations can result in callusing instead of root formation, which was observed to a small extent in T3. Therefore, a low-concentration, short-duration exposure to NAA appears optimal for rooting in softwood cuttings of *Valeriana jatamansi* Jones.

SUMMARY AND CONCLUSION

The present study, titled "Propagation of *Valeriana jatamansi* Jones through Cuttings", was carried out at the Faculty of Forestry, Sher-e-Kashmir University of Agricultural Sciences and Technology of Kashmir, during the autumn semester of 2024. The aim was to develop an effective vegetative propagation protocol using apical cuttings of *Valeriana jatamansi* Jones, a high-value medicinal herb that is currently listed as endangered due to overexploitation and habitat degradation (Maurya *et al*., 2017). A total of 100 cuttings were treated with three different concentrations of Naphthalene Acetic Acid (NAA): 50 ppm, 100 ppm, and 150 ppm, with each treatment replicated. The analysis was performed using OPSTAT software following a Completely Randomized Design (CRD). The cuttings were maintained in transparent glass beakers filled with distilled water (hydroponic conditions) and placed under partial shade. The water was changed every two days to maintain oxygen availability and prevent microbial growth.

Observations made after 30 days focused on four critical parameters: rooting percentage, number of roots per cutting, root length, and root diameter. The findings revealed that 50 ppm NAA for 30 minutes (T1D1) was significantly superior in promoting rooting success across all parameters. Cuttings treated with 50 ppm NAA for 30 minutes had the highest rooting percentage (100%), produced an average of five roots per cutting, and exhibited longer and thicker roots compared to higher

concentrations. These results are in close agreement with Bhatt *et al*. (2021) [11], who reported improved rooting in Valeriana jatamansi under low to moderate concentrations of NAA and IBA, and with Gautam *et al*. (2021) [8], who noted that 50 ppm NAA was optimal under hydroponic conditions for this species.

The highest rooting percentage (100%) was recorded in cuttings treated with 50 ppm NAA for 30 minutes (T1D1).

The study found that 50 ppm NAA for 30 minutes (T1D1) produced a significantly higher number of roots (mean = 5), while T2 (100 ppm) and T3 (150 ppm) recorded mean values of 1.11 and 1.22

Longer roots were observed in T3, the overall mean root length was highest in T1 (0.63 cm), suggesting that lower auxin concentration led to more uniform and healthier root development.

T1D1 (50 ppm NAA for 30 minutes) recorded the greatest mean root diameter (0.271 cm), indicating superior vascular development. T2 and T3 treatments showed a reduction in root diameter, with some roots appearing fragile and underdeveloped.

In visual observation the cuttings under 50 ppm NAA for 30 minutes (T1D1) appeared greener, turgid, and free from symptoms of stress throughout the 30-day observation period. In contrast, cuttings in higher concentration treatments began to show leaf chlorosis, wilting, callus formation, and tissue necrosis, especially in T3.

A low-concentration, short-duration exposure to NAA appears optimal for rooting in softwood cuttings of *Valeriana jatamansi* Jones.

The hydroponic setup proved advantageous for this experiment, allowing clean visibility of root formation and maintaining a disease-free environment.

CONCLUSION

In conclusion, this propagation protocol offers a simple yet reliable technique for nursery managers, conservation biologists, and medicinal plant cultivators aiming to multiply genetically uniform, high-quality planting material of *Valeriana jatamansi* Jones. Given its endangered status and pharmacological value, it is recommended that this method be integrated into medicinal plant conservation programs. Further studies may be undertaken to compare the effect of other rooting hormones (like IBA or IAA) and different rooting substrates (such as cocopeat or sand) under controlled environments to optimise field-level scalability.

REFERENCES

Bhattacharjee, S.K., Jaipur: Pointer Publishers (2000). Handbook of Aromatic Plants; pp. 458–9.
Google Scholar

Prakash, V. 1-2. Jodhpur, India: Scientific Publishers (1999). Indian Valerianaceae. A Monograph on Medicinally Important Family.
Google Scholar

Raina, R. and Srivastava, L.J. (1992). Floral Polymorphism in Valeriana jatamansi Jones. Indian *Journal of Plant Genetic Resources*, **5**, 93-94.
Google Scholar

Raina, A.P. and Negi, K.S. (2015) Essential Oil Composition of Valeriana jatamansi Jones from Himalayan Regions of India. *Indian Journal of Pharmaceutical Sciences*, **77**, 218-222.
Google Scholar

Raina, R and Srivastava, R.J. (1992). *Ind.J.Plant Sci*., **5**(2): 93 – 94
Google Scholar

Hooker, J.D. Flora of British India, Vol (III) 1881; pp. 213
Google Scholar

Kirtikar, K.R. and Basu, B.D. (1975). Indian Medicinal Plants. Bishen Singh Mahendra Pal Singh, Dehra Dun, pp. 311-312.
Google Scholar

Gautam, R.D., Kumar, A., Kumar, R., Chauhan, R., Singh, S., Kumar, M., Kumar, D., Kumar, A. and Singh, S. (2021). Clonal Propagation of Valeriana jatamansi Retains the Essential Oil Profile of Mother Plants: An Approach Toward Generating Homogenous Grade of Essential Oil for Industrial Use. Front. Plant Sci. **12**:738247. doi: 10.3389/fpls.2021.738247.
Google Scholar

De Klerk, G.-J., Van Der Krieken, W. and De Jong, J. C. (1999). The formation of adventitious roots: new concepts, new possibilities. In Vitro Cellular & Developmental Biology - Plant, **35**(3), 189–199.
Google Scholar

Hartmann, H. T., Kester, D. E., Davies, F. T. and Geneve, R. L. (2011). Hartmann & Kester's Plant Propagation: Principles and Practices (8th ed.). Prentice Hall.
Google Scholar

Bhatt, R., Asopa, P. P., Jain, R. and Kachhwaha, S. (2021). Efficient plant regeneration through callus culture in Hedychium spicatum / Trachyspermum copticum / Kodo millet.
Google Scholar

Baskaran, P. and Jayabalan, N. (2005). An efficient micropropagation system for Eclipta alba—A valuable medicinal herb. In Vitro Cellular & Developmental Biology - Plant, **41**(4), 532–539.
Google Scholar

Journal of Plant Development Sciences
Meerut, India

RESEARCH ARTICLE

EFFECT OF CROP GEOMETRY AND IRRIGATION FREQUENCY ON YIELD AND RESOURCE USE EFFICIENCY OF OKRA UNDER DRIP IRRIGATION

Nayan Kumar[1], Mukesh Kumar[2]*, Ram Naresh[2], Kapil[2], Kuldeep Singh[2] and Amandeep Singh[2]

[1,2]Department of Soil and Water Engineering, CCS HAU, Hisar
Email: mukeshdandi@yahoo.com

Received-18.03.2026, Revised-13.04.2026, Accepted-28.04.2026

Abstract: A field experiment was conducted during the summer season at the research farm of CCS Haryana Agricultural University, Hisar, to evaluate the effects of crop geometry and irrigation frequency on yield, irrigation water use efficiency (IWUE), and fertilizer use efficiency (FUE) of okra (*Abelmoschus esculentus* L.). The experiment was arranged in a split-plot design with three replications. Two crop geometries were assigned to main plots: normal geometry (plant spacing 30 cm, row spacing 45 cm, and lateral spacing 45 cm with one lateral per crop row) and paired-row geometry (plant spacing 30 cm, paired rows at 30 cm with 90 cm spacing between pairs and one lateral for each pair of rows). Four irrigation frequencies viz. daily irrigation, alternate-day irrigation, irrigation after three days, and irrigation after five days—were allotted to subplots. Crop geometry and irrigation frequency significantly influenced yield and resource use efficiencies. Normal geometry with daily irrigation produced the highest total yield (114.98 q ha^{-1}), IWUE (5.68 kg m^{-3}), and FUE (54.76 kg kg^{-1}), whereas the lowest values of yield (94.86 q ha^{-1}), IWUE (4.68 kg m^{-3}), and FUE (45.17 kg kg^{-1}) were observed under paired-row geometry with irrigation after five days. Overall, normal geometry resulted in higher average yield (106.74 q ha^{-1}) than paired-row geometry (102.85 q ha^{-1}). Similarly, daily irrigation recorded the highest mean yield (113.86 q ha^{-1}), IWUE (5.62 kg m^{-3}), and FUE (54.22 kg kg^{-1}), followed by alternate-day irrigation, irrigation after three days, and irrigation after five days.

Keywords: Irrigation water use efficiency, Fertilizer use efficiency, Paired row geometry

INTRODUCTION

Water availability for agriculture is decreasing globally, making efficient irrigation management essential for sustainable crop production. Researchers are increasingly focusing on methods that can produce higher yields using less water. Drip irrigation has emerged as an effective irrigation technique because it delivers water directly to the root zone, thereby improving irrigation water use efficiency (IWUE) and crop productivity.

Okra (*Abelmoschus esculentus*), commonly known as lady's finger or "bhindi" in India, is an important vegetable crop cultivated in tropical and warm temperate regions. According to Gopalan *et al.* (1989), 100 g of edible okra contains 1.9 g protein, 0.2 g fat, 6.4 g carbohydrates, 0.7 g minerals and 1.2 g fibre. Okra also contributes significantly to vegetable exports and has considerable potential as a foreign exchange earning crop. In India, Gujarat contributes the highest share (15.89%) of okra production, followed by West Bengal (13.93%), whereas Haryana contributes about 2.86%. The total production of okra in India during 2021–22 was about 5445 thousand tonnes (National Horticulture Board, 2022).

Irrigation management plays a crucial role in the growth and productivity of okra. Soil type, crop type, climatic condition, irrigation method and irrigation frequency are important factors affecting irrigation scheduling. Okra thrives under warm conditions but is sensitive to water stress, particularly during flowering and pod development stages. Studies have shown that frequent irrigation improves yield and water productivity in okra cultivation (Kumar *et al.*, 2016; Kumar *et al.*, 2023). Similarly, drip fertigation has been reported to save 20–61% water and increase yield by 13–76% compared with conventional irrigation methods (Sharma *et al.*, 2016).

Crop geometry is another important factor influencing crop growth and yield because it determines plant population, light interception, and efficient utilization of soil moisture and nutrients. Proper plant spacing allows better solar radiation interception and improves photosynthesis, ultimately enhancing crop productivity. Previous studies have indicated that wider spacing increases vegetative growth and yield per plant, whereas closer spacing increases yield per unit area (Ganjare *et al.*, 2013).

Although drip irrigation improves water use efficiency, its adoption is often limited due to the high initial cost, particularly the cost of lateral lines. Reducing the number of lateral lines by irrigating multiple crop rows with a single lateral can lower the system cost, but this may affect soil moisture distribution in the crop root zone. Modifying crop

*Corresponding Author

geometry, such as paired row planting, along with appropriate irrigation frequency may help maintain adequate soil moisture distribution while reducing the cost of drip irrigation systems.

Therefore, keeping in view the interaction between crop geometry and irrigation frequency, the present study was undertaken to evaluate their effect on irrigation water use efficiency, fertilizer use efficiency and yield of okra.

MATERIALS AND METHODS

Study Area

The experiment was conducted at the field laboratory of the Department of Soil and Water Engineering, CCS Haryana Agricultural University, Hisar, India, during February to June 2025. The study was carried out in brick-lined microplots of 2 m × 2 m size equipped with a drip irrigation system.

Soil Characteristics

Soil samples were collected from five randomly selected locations at 0–30 cm depth using a tube auger and mixed to form a composite sample for analysis. The soil of the experimental site was sandy loam in texture.

Experimental Design and Treatments

The experiment was laid out in a split plot design with two crop geometries and four irrigation frequencies, replicated three times.

Crop Geometry Treatments

- **G_1 – Normal geometry:** plant spacing 30 cm, row spacing 45 cm and lateral spacing 45 cm (one lateral per crop row).
- **G_2 – Paired row geometry:** plant spacing 30 cm, paired rows at 30 cm with 90 cm spacing between pairs (one lateral for each pair of rows).

Irrigation Frequency Treatments

- **I_1 – Daily irrigation**
- **I_2 – Alternate day irrigation**
- **I_3 – Irrigation after three days**
- **I_4 – Irrigation after five days**

Thus, eight treatment combinations (G_1I_1 to G_2I_4) were evaluated.

Crop Management Practices

Before sowing, 25 kg farmyard manure (FYM) per plot along with the recommended dose of fertilizers was incorporated into the soil. The recommended fertilizer dose for okra was 100 kg N, 60 kg P_2O_5 and 50 kg K_2O per hectare. Full doses of phosphorus and potassium and one-third of nitrogen were applied at sowing, while the remaining nitrogen was supplied through fertigation using the drip irrigation system.

Seeds of Hisar Unnat variety of okra were directly sown in the prepared plots on 25 February 2025. Gap filling was carried out after 10 days to maintain uniform plant population.

Weeds were controlled through regular hand weeding. During the experiment, pest infestation such as white fly and red-banded blister beetle and leaf shrinkage were observed. These were controlled by spraying recommended doses of carbendazim and monolik pesticides.

Irrigation Scheduling

Initially, irrigation was provided through a garden hose for 10 days for crop establishment. Afterwards irrigation was scheduled using the pan evaporation method based on 100% pan evaporation (PE). Meteorological parameters such as pan evaporation and rainfall during the experimental period were obtained from the Department of Agricultural Meteorology of the university.

Crop evapotranspiration was calculated as:

$$ET_c = K_c * K_p * CPE \quad \ldots(1)$$

Where,

K_c = Crop coefficient values

K_p = Pan coefficient (0.7)

CPE = cumulative pan evaporation

Crop coefficient of okra crop was taken from Patil and Tiwari, 2018.

The volume of water applied was calculated by using the following formula (Kaulage, 2017):

$$V = \frac{ET_C * L_S * E_S * W_a}{EU} \quad \ldots(2)$$

Where

V = volume of water per plant (L)

Ls = lateral spacing

Es = emitter spacing

Wa = wetted area factor (0.7)

EU = emission uniformity (90%)

Irrigation duration was determined by:

$$\text{Irrigation time (h)} = \frac{V}{q} \quad \ldots(3)$$

where q represents dripper discharge (L h^{-1}).

Soil Moisture Measurement

Soil samples were collected using a tube auger from depths of 0–15, 15–30, 30–45 and 45–60 cm at different distances from the dripper. Soil moisture content was determined using the gravimetric method by drying samples in an oven at 105°C for 24 hours.

Soil moisture content was calculated as:

$$\text{Moisture content (percent)} = \frac{W_1 - W_2}{W_2} * 100 \quad \ldots(4)$$

Where,

W_1 = weight of soil sample before drying (gm)

W_2 = weight of soil sample after drying (gm)

Crop Yield:

Total yield per plot was calculated by summing the weight of fruits obtained from successive harvests.

Efficiency Parameters

Irrigation Water Use Efficiency (IWUE) was calculated as:

$$\text{IWUE}(kg\ m^{-3}) = \frac{Weight\ of\ fruit\ (kg)}{Amount\ of\ water\ applied\ (m^3)} \quad \ldots(5)$$

Fertilizer Use Efficiency (FUE) was determined as:

$$\text{FUE}(kg\ kg^{-1}) = \frac{Weight\ of\ fruit\ (kg)}{Amount\ of\ fertilizer\ applied\ (kg)} \quad \ldots(6)$$

Statistical Analysis

The experimental data were statistically analyzed using split plot design analysis with the help of OPSTAT statistical software (Sheoran, 2010). Analysis of variance (ANOVA) was performed and treatment means were compared using the critical difference (CD) at the appropriate significance level.

RESULTS AND DISCUSSION

Crop yield: Table 1 represents the effect of crop geometry (G), irrigation frequency (I), and their two-way interactions on the average total yield (q ha^{-1}) of okra. Under normal geometry (lateral spacing 45 cm), the total yield recorded under daily irrigation was higher by 4.62, 9.69, and 14.35 percent compared with alternate day irrigation, irrigation after three days, and irrigation after five days, respectively.

Table 1. Effect of crop geometry (G) and irrigation frequency (I) and their two way interactions on average total yield (q ha^{-1}) of okra

G X I Mean table						CD(p= 0.05)
I / G	**I_1**	**I_2**	**I_3**	**I_4**	**Mean G**	G X I 2.37
G_1	114.98	109.65	103.83	98.47	106.74	
G_2	112.74	106.41	97.40	94.85	102.85	G 2.08
Mean I	113.86	108.03	100.62	96.66		I 1.27

Similar findings were reported by Haris *et al.* (2014), who observed that daily irrigation was more effective for improving okra production. In paired row geometry (lateral spacing 90 cm), the total yield under daily irrigation was higher by 5.61, 13.60, and 15.85 percent compared with alternate day irrigation, irrigation after three days, and irrigation after five days, respectively.

When comparing total yield under both crop geometries, normal geometry produced higher yields across the respective treatments. Normal geometry ensures a more uniform distribution of plants across the field, which contributes to greater cumulative yield. Madisa *et al.* (2014) also reported that wider spacing did not significantly increase fruit yield, while Maurya *et al.* (2013) indicated that closer spacing produced higher yield compared with wider spacing.

Among all treatment combinations, the maximum total yield (114.98 q ha^{-1}) was recorded in treatment G_1I_1, whereas the minimum yield (94.86 q ha^{-1}) was observed in treatment G_2I_4 (Figure 1). The interaction effect between crop geometry and irrigation frequency on the average total yield of okra was found to be statistically significant.

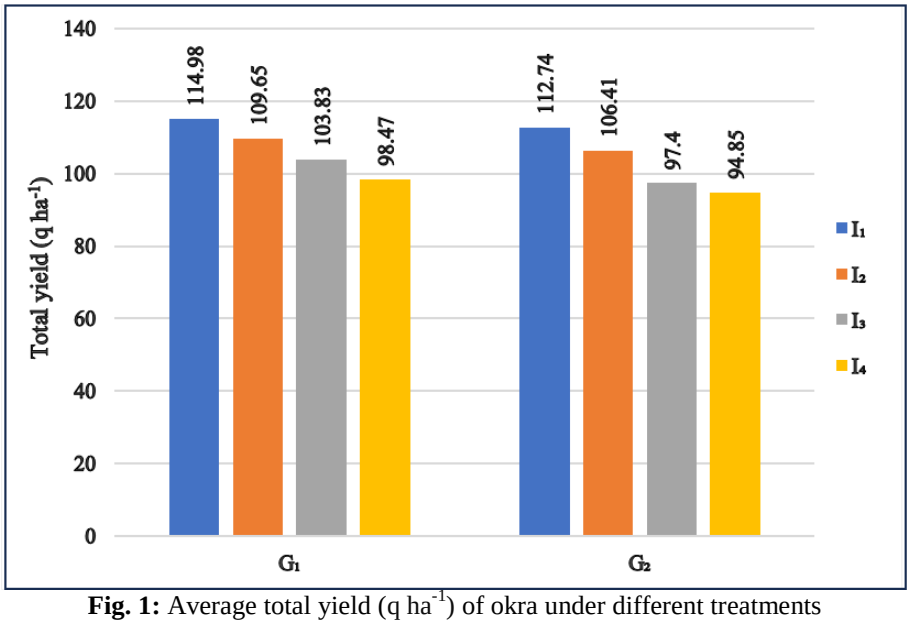

Fig. 1: Average total yield (q ha^{-1}) of okra under different treatments

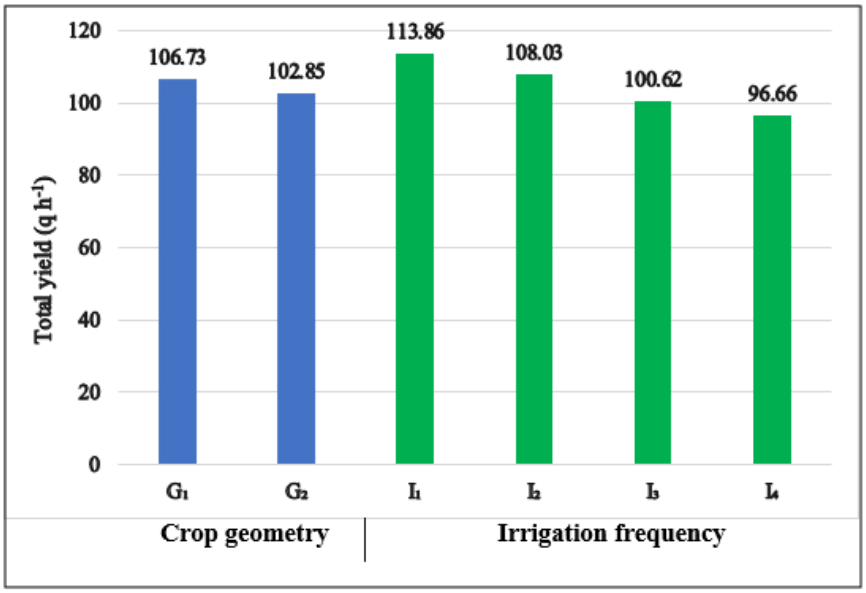

Fig. 2: Effect of crop geometry (G) and irrigation frequency (I) on average total yield (q ha^{-1}) of okra

Okra is generally cultivated during the summer season when temperatures remain high. Under such conditions, daily irrigation maintains an adequate soil water–air balance, which promotes better plant growth and may be responsible for higher yields under this irrigation frequency. The reduced yields under alternate day irrigation and irrigation after three and five days may be attributed to mild moisture stress during critical growth stages, caused by the vertical movement of water in the sandy soil of the study area.

The effect of crop geometry on average total yield of okra was statistically significant. Treatments with normal geometry recorded a higher average yield (106.74 q ha^{-1}) compared with paired row geometry (102.85 q ha^{-1}) (Table 1 and Fig. 2). Similarly, irrigation frequency significantly influenced the average total yield of okra. The highest yield was obtained under daily irrigation (113.86 q ha^{-1}), followed by alternate day irrigation (108.03 q ha^{-1}), irrigation after three days (100.62 q ha^{-1}), and irrigation after five days (96.66 q ha^{-1}) (Table 1 and Fig. 2).

Irrigation water use efficiency

Table 2 presents the effect of crop geometry (G), irrigation frequency (I), and their two-way interactions on irrigation water use efficiency (IWUE) of okra in terms of yield obtained per unit of water applied (kg m^{-3}) on a hectare basis. Since an equal amount of irrigation water was applied in all treatments, variations in IWUE were primarily due to differences in total yield. Therefore, higher yields corresponded to higher IWUE values.

Under both normal and paired row geometries, daily irrigation resulted in higher IWUE compared with alternate day irrigation, irrigation after three days, and irrigation after five days. This indicates that daily irrigation provides an optimal irrigation schedule for improving water productivity.

Table 2. Effect of crop geometry (G) and irrigation frequency (I) and their two way interactions on irrigation water use efficiency of okra

G X I Mean table						**CD (p= 0.05)**
I / **G**	**I_1**	**I_2**	**I_3**	**I_4**	**Mean G**	G X I 0.11
G_1	5.68	5.42	5.13	4.87	5.27	
G_2	5.57	5.25	4.81	4.68	5.08	G 0.10
Mean I	5.62	5.34	4.97	4.78		I 0.06

Figure 3 shows that the highest IWUE (5.68 kg m^{-3}) was observed in treatment G_1I_1, whereas the lowest IWUE (4.68 kg m^{-3}) was recorded in treatment G_2I_4. Similar results were reported by Jeelani *et al.* (2017). When comparing crop geometries, normal geometry consistently produced higher IWUE than paired row geometry at the corresponding irrigation frequencies. The interaction effect of crop geometry and irrigation frequency on IWUE at 90 DAS was also found to be statistically significant.

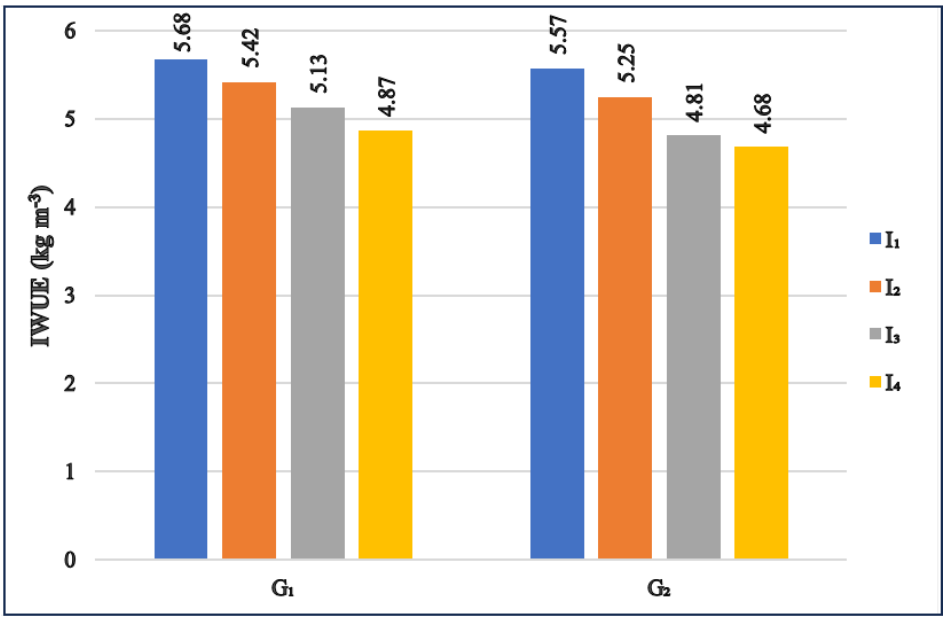

Fig. 3: Irrigation water use efficiency of okra under different treatments

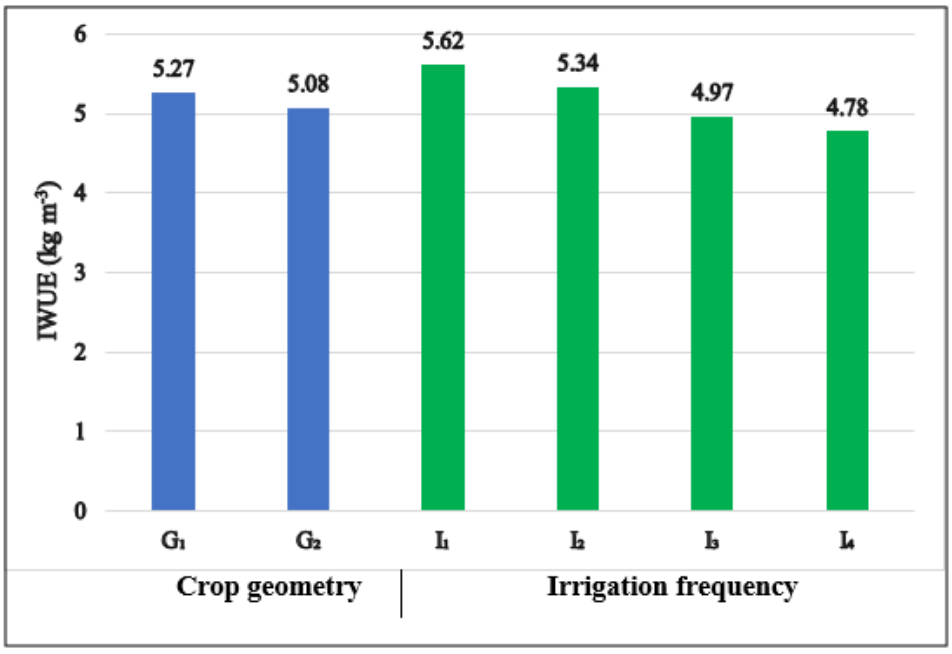

Fig. 4: Effect of crop geometry (G) and irrigation frequency (I) on irrigation water use efficiency of okra

The effect of crop geometry on average IWUE was statistically significant, with normal geometry recording higher IWUE (5.27 kg m^{-3}) compared with paired row geometry (5.08 kg m^{-3}) (Table 2 and Fig. 4). Irrigation frequency also had a significant effect on IWUE. The highest average IWUE was obtained under daily irrigation (5.62 kg m^{-3}), followed by alternate day irrigation (5.34 kg m^{-3}), irrigation after three days (4.97 kg m^{-3}), and irrigation after five days (4.78 kg m^{-3}) (Table 2 and Fig. 4).

Fertilizer use efficiency

Table 3 illustrates the effect of crop geometry (G), irrigation frequency (I), and their two-way interactions on fertilizer use efficiency (FUE) of okra, expressed as yield obtained per unit quantity of fertilizer applied (kg kg^{-1}) on a hectare basis. Since an equal amount of fertilizer was applied across all treatments, variations in FUE were mainly attributed to differences in total yield.

Table 3. Effect of crop geometry (G) and irrigation frequency (I) and their two way interactions on fertilizer use efficiency of okra

G X I Mean table						**CD (p= 0.05)**
I / **G**	**I_1**	**I_2**	**I_3**	**I_4**	**Mean G**	G X I 1.13
G_1	54.76	52.22	49.44	46.89	50.83	
G_2	53.68	50.67	46.38	45.17	48.98	G 1.02
Mean I	54.22	51.45	47.91	46.03		I 0.60

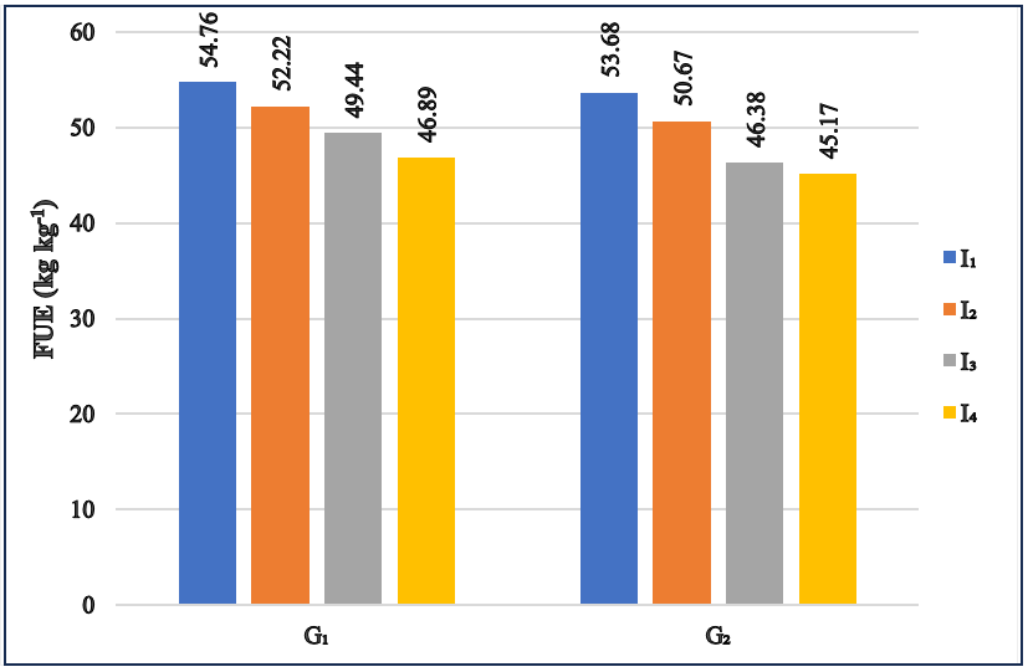

Fig. 5: Fertilizer use efficiency of okra under different treatments

Under both normal and paired row geometries, daily irrigation resulted in higher FUE compared with alternate day irrigation, irrigation after three days, and irrigation after five days, indicating that daily irrigation provides optimal conditions for nutrient utilization.

Figure 5 shows that the highest FUE (54.76 kg kg^{-1}) was recorded in treatment G_1I_1, whereas the lowest value (45.17 kg kg^{-1}) was observed in treatment G_2I_4. In comparison between crop geometries, normal geometry consistently showed higher FUE than paired row geometry at the corresponding irrigation frequencies. The interaction effect of crop geometry and irrigation frequency on fertilizer use efficiency of okra was also statistically significant.

The effect of crop geometry on average FUE was statistically significant, with normal geometry recording higher FUE (50.83 kg kg^{-1}) compared with paired row geometry (48.98 kg kg^{-1}) (Table 3 and Fig. 6). Varughese *et al.* (2014) and Arunadevi *et al.* (2023) also reported that single-row drip lateral geometry achieved higher yield compared with double-row drip lateral geometry with the same fertilizer application, mainly due to differences in plant density, root competition, and nutrient uptake efficiency.

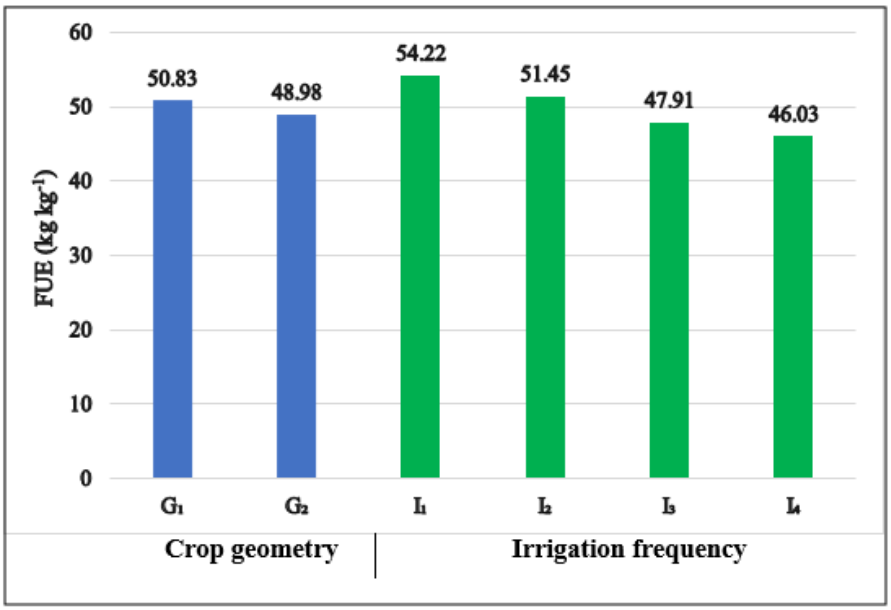

Fig. 6: Effect of crop geometry (G) and irrigation frequency (I) on fertilizer use efficiency of okra

Irrigation frequency also significantly affected fertilizer use efficiency. The highest average FUE was recorded under daily irrigation (54.22 kg kg^{-1}), followed by alternate day irrigation (51.45 kg kg^{-1}), irrigation after three days (47.91 kg kg^{-1}), and irrigation after five days (46.03 kg kg^{-1}) (Table 3 and Fig. 6). Higher irrigation frequency improves fertilizer use efficiency in okra by maintaining continuous nutrient availability, reducing nutrient losses, and maximizing pod yield per unit of fertilizer applied. In contrast, less frequent irrigation intervals may reduce FUE due to moisture stress periods and increased nutrient losses. Similar observations were also reported by Arunadevi *et al.* (2023).

CONCLUSIONS

The present study demonstrated that both crop geometry and irrigation frequency significantly influenced the yield, irrigation water use efficiency (IWUE), and fertilizer use efficiency (FUE) of okra under drip irrigation. Among the irrigation treatments, daily irrigation produced the highest total yield, IWUE, and FUE, whereas irrigation after five days resulted in the lowest values of these parameters. Higher irrigation frequency maintained favorable soil moisture conditions during the crop growth period, which enhanced plant growth and ultimately increased yield and resource use efficiency.

Crop geometry also showed a significant effect on okra performance. Normal geometry with a lateral spacing of 45 cm recorded higher yield, IWUE, and FUE compared with paired row geometry with 90 cm lateral spacing. The higher productivity under normal geometry may be attributed to more uniform plant distribution and improved utilization of water and nutrients.

The interaction between crop geometry and irrigation frequency was also found to be significant. The combination of normal geometry with daily irrigation (G_1I_1) resulted in the maximum yield (114.98 q ha^{-1}), IWUE (5.68 kg m^{-3}), and FUE (54.76 kg kg^{-1}), whereas the lowest values were recorded under paired row geometry with irrigation after five days (G_2I_4).

Therefore, the results indicate that maintaining normal crop geometry along with daily irrigation scheduling is the most effective strategy for improving yield and resource use efficiency of okra under drip irrigation conditions in sandy loam soils.

REFERENCES

Adeogun, E.O. (2016). Yield response of okra to irrigation frequency and amount in a sprinkler irrigation system. *Continental Journal of Agricultural Science*, **10**(2): 24–31.
Google Scholar

Arunadevi, K., Singh, M., Khanna, M., Mishra, A.K., Prajapati, V.K., Denny, F., Ramachandran, J. and Maruthi Sankar, G.R. (2023). Soil-matric-potential-based irrigation scheduling to increase yield and water productivity of okra. *Water*, **15**(24): 4300.
Google Scholar

Choudhary, S., Chandra, A. and Yadav, P.K. (2012). Effect of crop geometry on okra (*Abelmoschus esculentus*) cultivars under different irrigation levels and mulching. *Progressive Horticulture*, **44**(2): 276–280.
Google Scholar

Gopalan, C., Rama sastri, B.V. and Balasubramanian, S.C. (1996). *Nutritive Value of Indian Foods*. National Institute of Nutrition, Indian Council of Medical Research, Hyderabad, India.
Google Scholar

Haris, A.A., Kumar, S., Singh, A.K. and Rajan, K. (2014). Drip irrigation scheduling in okra (*Abelmoschus esculentus* L. Moench). *HortFlora Research Spectrum*. Volume **3** (3): pp 274-77.
Google Scholar

Jeelani, J., Katoch, K.K. and Sandal, S.K. (2017). Effect of drip fertigation levels on soil water dynamics, water use efficiency, yield and quality parameters of broccoli (*Brassica oleracea* L. var. *italica*) in wet temperate zone of Himachal Pradesh. *Indian Journal of Soil Conservation*, **45**(1): 96–104.
Google Scholar

Kaulage, P.P. (2017). Studies on growth and yield of onion crop under different moisture regimes with subsurface drip irrigation. *M.Sc. Thesis*, Mahatma Phule Krishi Vidyapeeth, Rahuri, Ahmednagar, Maharashtra, India.
Google Scholar

Kumar, N., Kumar, S., Duhan, D., Singh, A., Sidhpuria, M.S., Antil, S.K., Kumar, A. and Vikas, V. (2023). Production of subsurface drip-irrigated okra under different lateral spacings and irrigation frequencies. *Water SA*, **49**(2): 164–178.
Google Scholar

Kumar, S., Sanjay Kumar, S.K., Sharma, S.K., Rajpaul, R. and Ram Prakash, R.P. (2016). Effects of irrigation frequency and salinity under drip irrigation on okra (*Abelmoschus esculentus* L.). *Journal of Soil and Water Conservation*, **15** (2), 114-119.
Google Scholar

Madisa, M.E., Mathowa, T., Mpofu, C. and Oganne, T.A. (2014). Effects of plant spacing on the growth, yield and yield components of okra (*Abelmoschus esculentus* L.) in Botswana. *American Journal of Experimental Agriculture*, **6**(1): 7–14.
Google Scholar

Maurya, R.P., Bailey, J.A. and Chandler, J.S.A. (2013). Impact of plant spacing and picking interval on the growth, fruit quality and yield of okra (*Abelmoschus esculentus* L. Moench). *American Journal of Agriculture and Forestry*, **1**(4): 48–54.
Google Scholar

National Horticulture Board (NHB). (2022). *Indian Horticulture Database 2021–22*. Ministry of Agriculture and Farmers Welfare, Government of India, Gurugram, Haryana. Available at: https://nhb.gov.in
Google Scholar

Sharma, P., Kaushal, A., Singh, A. and Garg, S. (2016). Growth and yield attributes of okra under influence of drip irrigation. *Journal of Engineering Research and Applications*, **6**(2): 85–91.
Google Scholar

Sheoran, O.P., Tonk, D.S., Kaushik, L.S., Hasija, R.C. and Pannu, R.S. (1998). Statistical software package for agricultural research workers (OPSTAT). CCS Haryana Agricultural University, Hisar, India. *www.hau.ac.in*
Google Scholar

Varughese, A., Menon, J.S. and Mathew, E.K. (2014). Effect of fertigation levels and drip system layout on performance of okra under plastic mulch. *Journal of Agricultural Engineering*, **51**: 28–32.
Google Scholar

Journal of Plant Development Sciences
Meerut, India

RESEARCH ARTICLE

EFFECT OF CLUSTER FRONT LINE DEMONSTRATIONS ON ENHANCEMENT OF YIELD AND ECONOMICS OF MUSTARD CULTIVATION IN DIDWANA-KUCHAMAN DISTRICT OF RAJASTHAN

A.S. Jat*[1], S.D. Bamboriya[2] and S.R. Kumawat[3]

[1]Krishi Vigyan Kendra, Maulasar, Nagaur-II, Agriculture University, Jodhpur
[2]Department of Agronomy, SKNAU, Jobner, (Rajasthan)
[3]Directorate of Extension Education, Agriculture University, Jodhpur, Rajasthan, India
Email: dr.asjat@gmail.com

Received-23.03.2026, Revised-10.04.2026, Accepted-27.04.2026

Abstract: Under centrally sponsored programme on oilseed production technology under NFSM schemes, KVK Maulasar conducted 815demonstrations on different varietyof mustard during *Rabi*, 2016-17 to 2023-24. The critical inputs were identified in existing production technology through discussion with farmers and on the basis of soil sampling. Lack of plant protection measures were the predominant identified causes of low productivity of oilseed crop in district Didwana-Kuchaman of Rajasthan. In the same sequence the other parameters like technological impact, economical impact and extension gap were analyzed for impact assessment of cluster frontline demonstrations (CFLDs) on mustard crop. The results of eight consecutive years study revealed that the average yield under demonstration plots was obtained 17.26 q/ha as compared to 14.63 q/ha in farmer plots with average 18.10 % increase in yield. The average technology gap, extension gap & technological index were found 636 kg/ha, 264 kg/ha and 26.93 percent, respectively. Further, data showed that the average additional cost of cultivation (Rs. 2011/ha) under integrated crop management demonstrations and has fetched additional net returns of Rs. 10896 per hectare with incremental benefit: cost ratio of 0.26. The results clearly indicate the positive effect of CFLDs over the existing practices.

Keywords: Economic analysis, Extension gap, Frontline demonstration, Mustard, Yield

INTRODUCTION

Mustard (*Brassica juncea* L.) is an important oilseed crop in India. Rapeseed- mustard is the major source of income especially even to the small and marginal farmers in rainfed areas because of its low water requirement (80-240mm) so it fits well in the rainfed cropping system. Its seed contain 35-40% oil and 16-22% protein content and high level of amino acids. The oil of mustard possesses a sizable amount of erucic acid (38-57%). Protein content in rapeseed and mustard normally range between 24-30% on the basis of whole seed basis and between 35-40% on the meal basis. The leaves of young plants are used in human diet as a green vegetable. The oilseed Brassica usually contains 4.7-13% linolenic acid and 27% oleic acid and high nutritive value required for human health.

Indian mustard *Brassica juncea*is predominantly cultivated in Rajasthan, U.P. Haryana, M.P. and Gujarat [7].Rajasthan is the undisputed mustard powerhouse of India, contributing over 40-45 per cent of the country's total output. The state cultivated4.55 million hectares of mustard, yielding 6.68 million tonnes of produce with average productivity of 1468 kg/ha during the year 2022-23 [1].

*Corresponding Author

The improved technology packages were also found to be financially attractive. Yet, adoption level of several components of improve technology were low, emphasizing the need for better dissemination.Keeping the above points in view the FLDs on mustard using new crop production technology was started with the objectives of showing the productive potentials of the new production technology under real farm situation over the locally cultivated mustard crop and to know the varietal replacement of oilseed crops and its horizontal spread due to FLDs.

MATERIALS AND METHODS

The present study was carried out in the Didwana-Kuchaman district which is a part of Nagaur district and located on the North-western part of Rajasthan state and lies at 27°20'N latitude and 73°74' E longitude with an altitude of 302 m above the mean sea level. Cluster frontline demonstrations were conducted during consecutiverabi seasons from 2016-17 to 2023-24at the farmers fields of different villages of Didwana-Kuchaman district in Transitional plain of Inland drainage zone of Rajasthan. In this study, total815 farmers were selected from aforesaid block during consecutive

years and cluster front line demonstrations were conducted on total 332 ha area. All the technological intervention was taken as per prescribed package and practices for improved varieties of mustard crop (Table 1). The grain yield, cost of cultivation, net returns and additional return parameters were recorded (Tables 2-4). Assessment of gap in adoption of recommended technology was done before laying out FLD's through personal discussion with selected farmers. The training was organized for selection of farmer's and skilled development about detailed technological intervention with improved package and practice for successful mustard cultivation. Scientists visited regularly demonstrated fields and farmer's field also. The feedback information from the farmers was also recorded for further improvement in research and extension programmes. The extension activities i.e. training, scientist's visits and field days were organized at the cluster frontline demonstration sites. The basic information were recorded from the farmer's field and analyzed to comparative performance of demonstrated plot and local check. The technology gap, extension gap and technology index were calculated using the following formulae given by [8].

Extension gap = Demonstrated yield- Farmer's practice yield

Technology gap= Potential yield- Demonstration yield

Additional return= Demonstration return- farmer's practice return

Technology index=

$$\frac{\text{Potential yield} - \text{Demonstration yield}}{\text{Potential yield}} \times 100$$

The satisfaction level of partner farmers for the performance of improved technology demonstrated was also assessed. In all, 815 partner farmers were selected to measure satisfaction level of farmers for the performance of improved technological package demonstrated. The selected respondents were interviewed personally with the help of a pre-tested and well structured interview schedule and Client Satisfaction Index was calculated as below.

Client satisfaction index = (Individual score obtained/ Maximum score possible) x 100

The data collected were tabulated and analyzed to interpret the results. The economic-parameters (gross return, net return and B: C ratio) were worked out on the basis of prevailing market prices of inputs and Minimum Support Prices of outputs.

Table1. Detail of package and practices for mustard cultivation

S. No.	Technological intervention	Farmer's practice	Recommended Practice (FLD's)
1.	Variety	Bio-902, PM-26, PM-28, Pioneer 45S46, Pioneer 45S42,	NRCHB-101, NRCDR-2, DRMRIJ-31, RH-725, DRMR 1165-40
2.	Seed rate (kg/ha)	4-5	3.5-4.5
3.	Seed treatment	Seed treatment with Carbendazim 2g/kg seed	Metalaxyl 35 SD @ 6.0 g/kg+ Imidacloprid 70 WS 5 g/kg seed and *Azotobacter +PSB* culture@ 20 g/kg seed
4.	Soil treatment	No soil treatment	Soil treatment by *Trichoderma* spp. @ 2.5 kg/ha (mixed with 100 kg FYM)
5.	Spacing	30x10 cm	30x10 cm
6.	Time of Sowing	October-November	Second fortnight of October
7.	Nutrient management	Imbalance use of fertilizers	Balanced use of fertilizers (60 kg N + 30 kg P_2O_5 + 25 kg $ZnSO_4$/ha)
8.	Weed management	One hand weeding at 20-30 DAS	Use of Oxadiargyl @ 90 g *a.i.* or Pendimethalin 0.75 kg *a.i*/ha at 1-2 DAS + one hand weeding at 25-30 DAS
9.	Plant protection measures	Aphid- Dimethoate 30% E.C. @ 875 ml/ha White rust- Mancozeb @1.0 kg/ha.	Aphid-Dimethoate 30 E.C. @ 875 ml/ha or Thiomethoxam 25 WG @ 100 g/ha or Imidacloprid @ 150 ml/ha. White rust-Metalaxyl 8%+ Mancozeb 64% @ 1.0 kg/ha.

Table 2. Effect of Front Line Demonstrations on seed yield of mustard

FLD Conducted year	Area (ha)	No. of Demonstrations	Variety	Demonstrated plot yield (q/ha)	Local Check plot yield (q/ha)	Yield increased over local check (%)
2016-17	30	60	NRCDR-02	17.63	16.00	10.19
2017-18	12	30	NRCHB-101	17.51	15.50	12.97
2018-19	30	75	DRMRIJ-31	19.10	15.75	21.27
2019-20	120	300	DRMRIJ-31	18.00	14.30	25.87
2020-21	80	200	RH-725	17.70	14.50	22.07
2021-22	20	50	RH-725	17.60	14.60	20.55
2022-23	20	50	DRMR 1165-40	15.17	13.07	16.07
2023-24	20	50	DRMR 1165-40	15.40	13.30	15.79
Total	**332**	**815**	**Average**	**17.26**	**14.63**	**18.10**

Table 3. Effect of Front Line Demonstrations on Economics of mustard cultivation

FLD	Cost of cultivation (Rs/ha)		Gross return (Rs/ha)		Net Return (Rs/ha)	
Conducted year	Demonstrated plot	Local Check plot	Demonstrated plot	Local Check plot	Demonstrated plot	Local Check plot
2016-17	24200	22732	64297	58352	40097	35620
2017-18	25500	24080	71437	63237	45937	39157
2018-19	27600	25300	85874	70812	58274	45512
2019-20	28100	26550	85644	68039	57544	41489
2020-21	29650	27500	88810	72754	59160	45254
2021-22	30400	28200	92268	76541	61868	48341
2022-23	31950	29600	85619	73767	53669	44167
2023-24	34750	32100	93909	81103	59159	49003
Average	**29019**	**27008**	**83482**	**70576**	**54463**	**43568**

Table 4. Effect of Front Line Demonstrations on Additional economic performance of mustard

Conducted year	Additional cost in demonstrations (Rs./ha)	Additional return from demonstrations (Rs./ha)	B:C Ratio in demonstrations (Rs./ha)	B:C Ratio in Local Check plot
2016-17	1468	4477	2.66	2.57
2017-18	1420	6780	2.80	2.63
2018-19	2300	12762	3.11	2.80
2019-20	1550	16055	3.05	2.56
2020-21	2150	13906	3.00	2.65
2021-22	2200	13528	3.04	2.71
2022-23	2350	9502	2.68	2.49
2023-24	2650	10156	2.70	2.53
Average	**2011**	**10896**	**2.88**	**2.62**

RESULTS AND DISCUSSION

Effect on yield of mustard:

The performance of mustard crop owing to the adoption of improved technologies was assessed over a period of eight years and is presented in Table 2. Results of 815 cluster front line demonstrations showed that, the integrated crop management practice in mustard recorded 18.10 per cent increase in the average yield as compared to the farmers practice (14.63 q/ha). The seed yield of demonstration plots was higher as compared to farmers practice due to high yielding varieties grown under integrated crop management practices. Similar yield enhancement in different crops in front line demonstration has been documented by Balai *et al.* (2012), Choudhary *et al.*(2018), and Kirar *et al.* (2018). The results clearly indicated the positive effect of CFLDs over the existing practices toward enhancing the yield of mustard in the study area due to use of high yielding varieties, timely sowing, INM, IWM, plant protection etc.

Effect on Extension gap, Technology gap and Technology index:

The data on extension gap, technology gap andtechnology index are presented in Figure-1. The average extension gap of 2.64q/ha was recorded in mustard. This emphasized the need to educate the farmers through various means for the adoption of improved agricultural production to reverse the trend of wide extension gap.

The average value for technology gap was 6.36q/ha which reflected the farmer's cooperation in carrying out such demonstrations with encouraging results in subsequent years. The technology gap observed may be attributed to the dissimilarity in soil fertility status and weather conditions.

The technology index showed the feasibility of the evolved technology at the farmer's fields and the lower is the value of technology index, more the feasibility of the technology demonstrated as such lower value of index 26.93 percent exhibited the feasibility of technology demonstrated. The results of the present study are in consonance with the findings of Ahmad *et al.,* (2013), Kirar *et al.,* (2018) and Singh *et al.,* (2019).

Effect on Economic performance:

The economics of the data regarding cost of cultivation, gross return, net return, additional cost, additional return and benefit: cost ratio were analyzed and presented in Table-3 and 4.

Cost of cultivation, Gross and Net returns:

The economic analysis of the data (Table-3) revealed that mustard under cluster front line demonstrations recorded average cost of cultivation (Rs. 29019), gross return (Rs. 83482) and net returns (Rs. 54463) per hectare, which was 7.45, 18.29 and 25.01 per cent higher as compared to the local check, respectively. The findings of the present study are in line with the findings of Choudhary *et al.,* (2018) and Kirar *et al.,* (2018).

Additional Cost of cultivation, Return and B: C Ratio:

Further, data (Table 4) shows that the average additional cost of cultivation (Rs. 2011/ha) under integrated crop management demonstrations and has yielded additional net returns of Rs. 10896 per hectare with incremental benefit: cost ratio of 0.26.

The results suggested that higher profitability and economic viability of mustard demonstrations under local agro-ecological situation. This might be due to higher production under CFLDs as compared to the prevailing farmers practice in all the years.

Farmer's satisfaction:

The extent of satisfaction level of respondent farmers over performance of demonstrated technology was measured by Client Satisfaction Index (CSI) and results presented in Figure-2. It is observed that majority of the respondent farmers expressed high (53.62%) to the medium (33.01%) level of satisfaction regarding the performance of CFLDs, whereas, very few (13.37%) of respondents expressed lower level of satisfaction. The higher to medium level of satisfaction with respect to performance of demonstrated technology indicate stronger conviction, physical and mental involvement of in the front line demonstrations which in turn would lead to higher adoption. The results are in close conformity with the results of Dhaka *et al.* (2010).

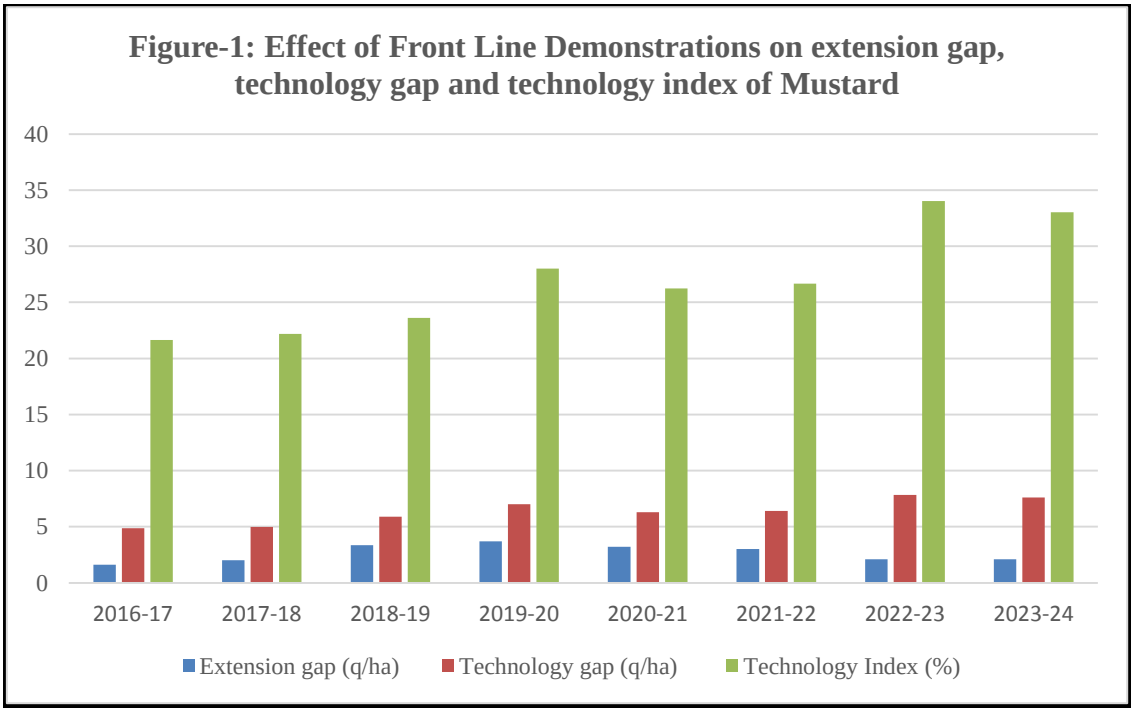

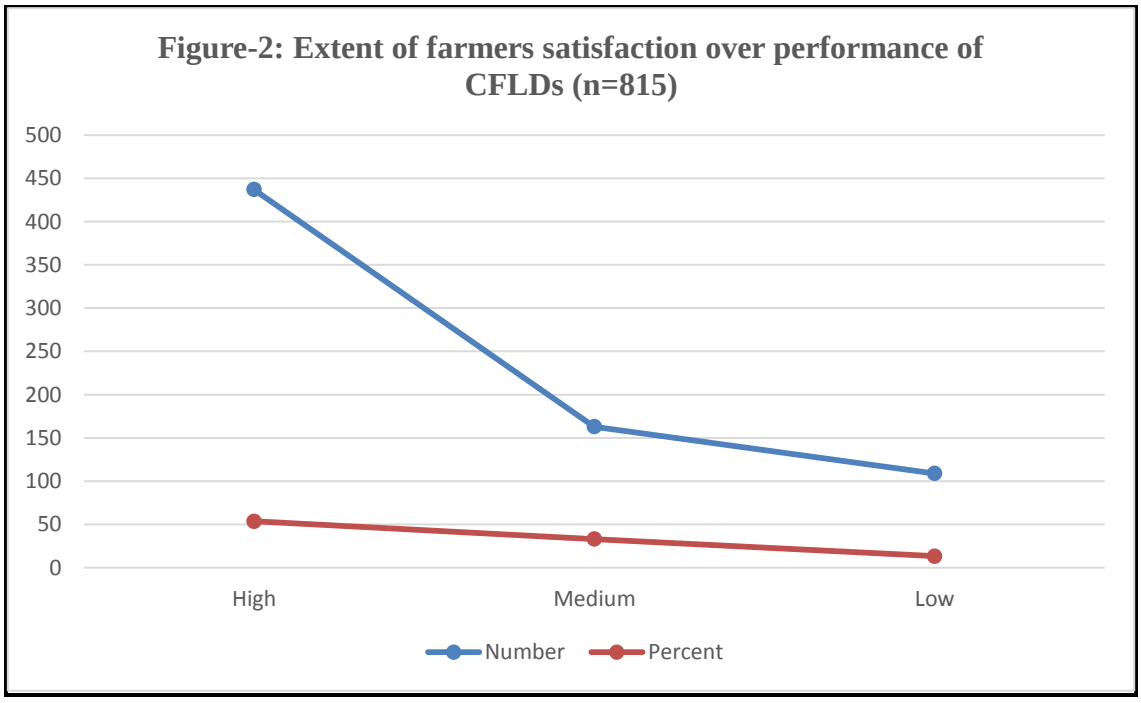

CONCLUSION

From the findings of present study, it can be concluded that use of latest technologies of mustard cultivation can reduce the technology gap to a considerable extent resulting in to increased productivity of mustard in the area. It requires collaborative extension efforts to enhance adoption level of location and crop specific technologies among of the farmers for bridging these gaps. Therefore, extension agencies in the area need provide proper technical support to the farmers through various education and extension methods for better mustard production in the area.

ACKNOWLEDGEMENT

Authors are thankful to ICAR, New Delhi for providing financial assistance for conducting frontline demonstrations on mustard crop and Agricultural Technology Application Research Institute (ATARI), Zone-II, Jodhpur as well as Directorate of Extension Education, Agriculture University, Jodhpur for proper guidance.

REFERENCES

Agricultural Statistics, Directorate of Economics and Statistics, Rajasthan (2022-23). Page. 22-29.
Google Scholar

Ahmad, A., Guru, P. and Kumar, R.(2013). *Indian Research Journal of Extension Education*, **12**(1):117.119.
Google Scholar

Balai, C.M., Meena, R.P., Meena, B.L. and Bairwa, R.K.(2012). *Indian Research Journal of ExtensionEducation*, **12** (2): 113-116.
Google Scholar

Chaudhary, R.P., Choudhary, G.K., Prasad, R., Singh, R. and Chaturvedi, A.K.(2018). *International Journal of Current Microbiology and Applied Sciences*, Special Issue-**7**: 4737-4742.
Google Scholar

Dhaka, B. L., Meena, B. S. and Suwalka, R. L.(2010). *Journal of Agriculture Science*, **1**(1): 39-42.
Google Scholar

Kirar, B.S., Jaiswal, R.K., Singh, R.P. and Kirar, N.S.(2018). *International Journal of Chemical Studies*,**6**(3): 3251-3253.
Google Scholar

Singh, J.B., Singh, N.K. and Tripathi, C.K.(2019). *Global Journal for Research Analysis*, **8**(1):17-19.
Google Scholar

Samui, S. K., Maitra, S., Roy, D. K., Mondal, A. K. and Saha, D.(2000). *Journal of Indian Society of Coastal AgriulturalResesearch*,**18** (2):180-183.
Google Scholar